

Copyright Warning & Restrictions

The copyright law of the United States (Title 17, United States Code) governs the making of photocopies or other reproductions of copyrighted material.

Under certain conditions specified in the law, libraries and archives are authorized to furnish a photocopy or other reproduction. One of these specified conditions is that the photocopy or reproduction is not to be “used for any purpose other than private study, scholarship, or research.” If a user makes a request for, or later uses, a photocopy or reproduction for purposes in excess of “fair use” that user may be liable for copyright infringement,

This institution reserves the right to refuse to accept a copying order if, in its judgment, fulfillment of the order would involve violation of copyright law.

Please Note: The author retains the copyright while the New Jersey Institute of Technology reserves the right to distribute this thesis or dissertation

Printing note: If you do not wish to print this page, then select “Pages from: first page # to: last page #” on the print dialog screen

The Van Houten library has removed some of the personal information and all signatures from the approval page and biographical sketches of theses and dissertations in order to protect the identity of NJIT graduates and faculty.

ABSTRACT

The Flow Approach to Swept Volume

by

Haitao Jiang

In this thesis, a method for representing swept volume based on the sweep differential equation and sweep vector field flow is developed. This method can be used to determine the boundary representation of a swept volume generated by any polygonal object undergoing a general smooth 2-D sweep. For any given sweep and object, a set of candidate boundary points is computed using a selection criterion based on vector field behavior. The set of candidate boundary points is then trimmed in order to obtain the true boundary of the swept volume. This trimming procedure is based on some simple topological principles and it utilizes the concept of extended sweep. This method is more general and efficient than existing approaches (e. g. it can readily deal with the cases in which the swept volume area has “holes”) and can easily be extended to 3-D sweeps; the 3-D extension is discussed but only briefly. Several examples are given to illustrate the implementation of the prototype software for 2-D sweeps which has been developed in conjunction with this research.

Keywords: Swept volume, Geometric modeling, NC machining

THE FLOW APPROACH TO SWEEP VOLUME

by
Haitao Jiang

A Thesis
Submitted to the Faculty of
New Jersey Institute of Technology
in Partial Fulfillment of the Requirements for the Degree of
Master of Science

Department of Mathematics

January, 1993

APPROVAL PAGE

THE FLOW APPROACH TO SWEEP VOLUME

Haitao Jiang

Dr. Denis Blackmore, Thesis Advisor
Professor of Mathematics, NJIT

Dr. Ming Leu, Committee Member
Professor of Mechanical Engineering
and Sponsored Chair in Manufacturing/Productivity, NJIT

Dr. Jonathan Luke, Committee Member
Assistant Professor of Mathematics, NJIT

BIOGRAPHICAL SKETCH

Author: Haitao Jiang

Degree: Master of Science in Applied Mathematics

Date: January, 1993

Undergraduate and Graduate Educations:

- Master of Science in Applied Mathematics,
New Jersey Institute of Technology, Newark, NJ, 1993
- Master of Engineering in Computer Engineering,
Wuhan Institute of Hydraulic & Electrical Engineering,
Wuhan, P. R. China, 1990
- Bachelor of Engineering in Computer Engineering,
Wuhan Institute of Hydraulic & Electrical Engineering,
Wuhan, P. R. China, 1987

Major: Applied Mathematics

This thesis is dedicated to
My wife Qing Yan

ACKNOWLEDGMENT

I would like to express my sincere gratitude to professor Denis Blackmore, my graduate advisor who introduced me into this interesting problem. I owe a lot to him for his constant guidance, encouragement, patience, and help in turning my ideas into rigorous mathematical expressions and proofs. He also helps me a lot on non-academic affairs; my thanks to him are beyond my words.

Thanks are also due to professor M. C. Leu of the Department of Mechanical and Industrial Engineering for his valuable insights into the problems. Also, I would like to express my special thanks to professor J. Luke of the Department of Mathematics, who was always willing to help me on the programs and the machine environments.

My thanks to Mr. Kyung Geun Pak, who is a member of our research team, for his ideas and good explanations of NC machining and robotics during our meetings. Also, I would like to thank my friends: Xiaoming Xiong, Kang Wu, Feng Bao, Fei Yu, Yongchun Liu, Chen Xu, Song Chen, Mingfu Fang and all the others, for their friendship and help on different aspects of this project.

The author was supported by an NJIT research assistantship and NSF Grant DDM-9114385 during the course of this research. This support is gratefully acknowledged.

TABLE OF CONTENTS

Chapter	Page
1 INTRODUCTION	1
1.1 Literature Survey	1
1.2 Envelope Theory Approach	3
2 THEORETICAL PRELIMINARIES	13
3 THE THEORY OF THE SWEEP FLOW APPROACH	18
3.1 The General Evaluation Procedure	18
3.2 The Selection of Candidate Boundary Points	19
3.3 The Global Trimming Procedure for the Candidate Boundary Points ..	27
4 IMPLEMENTATION OF PROTOTYPE SOFTWARE IN 2-D SPACE	34
4.1 Overview of the Whole Process	35
4.2 Implementation of Candidate Points Selection Procedure	37
4.3 Implementation of Trimming Procedure	42
4.4 Some Examples	47
5 SOME IDEAS ON 3-D EXTENSIONS	64
6 CONCLUSIONS	68
APPENDIX A: PROOF OF THE ALGORITHM 4.1	70
REFERENCES	73

LIST OF FIGURES

Figure	Page
1 Envelope of a family of circles whose centers are along the x axis	5
2 Swept volume of a line segment undergoing a 2-D sweep	8
3 Envelope curve of the swept volume of a line segment	9
4 The global nature of the sweep process	20
5 Illustration of partition of the boundary	23
6 Global trimming procedure from extended sweep point of view	28
7 A 2-D example of singular case in the global trimming	31
8 The object in example 4.1	38
9 The swept volume in example 4.1	39
10 The candidate boundary points of example 4.1	43
11 Deciding whether a point is inside a polygon or not	46
12 The boundary points after global trimming of example 4.1	48
13 The final boundary of the swept volume of example 4.1	49
14 The swept volume of example 4.2	52
15 The candidate boundary points of example 4.2	53
16 The boundary points after global trimming of example 4.2	54
17 The boundary representation of the swept volume of example 4.2	55
18 The swept volume of example 4.3	56
19 The candidate boundary points of example 4.3	57
20 The boundary points after global trimming of example 4.3	58
21 The boundary representation of swept volume in example 4.3	59
22 The swept volume of example 4.4	60
23 The candidate boundary points of example 4.4	61
24 The boundary points after global trimming of example 4.4	62

25	The boundary representation of swept volume in example 4.4.....	63
----	---	----

CHAPTER 1

INTRODUCTION

1.1 Literature Survey

The swept volume is the set of points in Euclidean space traversed by a solid object undergoing a continuous Euclidean motion (sweep). Evaluation and representation of the swept volume of an object undergoing a rigid-body motion have many important applications in manufacturing automation, such as NC machining program verification, the path planning and manipulation of robots, etc.

There are several different solid modeling schemes for representing swept volumes on which evaluation procedures are based. A representation scheme should, in principle, contain all the geometric properties of the swept volume and automatically support a variety of applications. The selection of the representation scheme really depends on the applications for which it is intended; however, here we shall discuss only the two most commonly used schemes, which are constructive solid geometry and boundary representation.

- **Constructive Solid Geometry**

Constructive Solid Geometry (CSG) represents an object as Boolean combinations of *primitives* through operators called *regularized set union* (\cup^*), *intersection* (\cap^*), *difference* ($-^*$) and *complement* (c^*) [16]. The regularized set operators are extensions of the corresponding standard set operators, followed by a *regularization process*, which guarantees that an operation on valid solids results also in a valid solid. The primitives are the basic geometric objects on which different solids are built: the commonly used primitives include blocks, cylinders, cones and tori. The different primitives that a system can support directly decide the capacity of the system. CSG representation is essentially a

binary tree, whose root represents the entire solid, whose leaves are the primitives, and whose internal nodes are the regularized Boolean operations or rigid motions. Each internal node can also be considered to represent a solid which is the part of the entire solid obtained by applying the operation to its two sons. The main advantage of this scheme is that it corresponds closely to how the solid is actually constructed; however, much of the geometric information is in implicit form which requires the application programs to have some procedures for evaluating the geometric properties of the solid in this representation.

- **Boundary Representation**

As indicated by its name, Boundary Representation represents a solid by its boundary. The boundary should be expressible as a set of surfaces. If the underlying manifolds of these surfaces are difficult to determine, they are often approximated by a set of patches whose underlying manifolds are known. Two of the most commonly used patches are the planar patch (which is a line segment in 2-D space) and the bicubic patch. The main advantage of this scheme is that the boundary is expressed explicitly, as is all of the important geometric information, which makes Boundary Representation very useful for a variety of applications.

For the details and other solid modeling schemes, readers can refer to [17], [18], [19].

Much research has been done in order to evaluate the swept volume and obtain various solid geometric representations. Sungertekin and Voelcker did a feasibility study of using the PADL solid modeling system for simulation of NC programs (see [22]). Since PADL uses Constructive Solid Geometry (CSG) to represent solids, the cost of simulation is proportional to the fourth power of the number of tool movements and this is computationally prohibitive. Drysdale, Jerard and their students

used surface discretization and normal vectors to indicate the geometry (see [8], [10]); this is computationally more efficient than the CSG representation since its computation time is linearly proportional to the number of cutting movements. However, in this method the cutter swept volume is not explicitly represented; instead the points of intersection between the lines of surface normals and the cutter swept volume are computed. The method of employing envelope theory to model the swept volume using boundary representation has been studied by K. K. Wang, W. P. Wang, Sambandan, etc. (see [20], [23], [24]). Due to its close relationship with our research, we will briefly introduce the basic theory of the envelope method and describe the most recent work being done in this area in the following section.

1.2 Envelope Theory Approach

There are many equivalent ways to define the envelope of a family of curves:

Definition 1.1 If there is a curve to which some of the curves of a family $F(\mathbf{x}, t) = 0$ are tangent and if the point of tangency describes a curve as t varies, the curve is called the *envelope* (or part of the envelope if there are several such curves) of the family $F(\mathbf{x}, t) = 0$.

Definition 1.2 If we have a family of surfaces (or curves), then the *envelope* can be defined as another surface (or curve) that is tangent at each of its points to some member of the family [6].

It is also useful to think of an envelope as the limit of the points in which neighboring curves of the family intersect; this is sometimes taken as the definition of the envelope:

$$\lim_{\Delta t \rightarrow 0} \frac{1}{\Delta t} [F(\mathbf{x}, t) - F(\mathbf{x}, t + \Delta t)] = \lim_{\Delta t \rightarrow 0} F_t(\mathbf{x}, t + \theta \Delta t) = F_t(\mathbf{x}, t) = 0$$

To find the envelope of a family, it is easy to prove from the definition that the points on the envelope must satisfy the following two conditions:

$$F(\mathbf{x}, t) = 0 \quad (1)$$

$$F_t(\mathbf{x}, t) = 0 \quad (2)$$

where F_t denotes the partial derivative of F with respect to t .

Once we have these two equations, the equation of the envelope of the family $F(\mathbf{x}, t) = 0$ may be found by solving them simultaneously to find a parametric equation $\mathbf{x} = \phi(t)$ or by eliminating t from the equations to obtain the envelope equation in the form of $\Phi(\mathbf{x}) = 0$.

Example 1.1 Find the envelope of $F(\mathbf{x}, t) = (x - t)^2 + y^2 - 1 = 0$.

We compute $F_t(\mathbf{x}, t) = -2(x - t) = 0$. By eliminating t from these two equations, we obtain $y = \pm 1$, which is the equation of the envelope. This example is shown in Figure 1.

The above concepts and methods can be easily extended to finding the envelope of a family of curves with k parameters, say $F(\mathbf{x}, t_1, t_2, \dots, t_k) = 0$. For example, if the family has 2 parameters, $F(\mathbf{x}, t_1, t_2) = 0$, the conditions for the envelope are:

$$F(\mathbf{x}, t_1, t_2) = 0 \quad (3)$$

$$F_{t_1}(\mathbf{x}, t_1, t_2) = 0 \quad (4)$$

$$F_{t_2}(\mathbf{x}, t_1, t_2) = 0 \quad (5)$$

If we want to apply the envelope theory directly to the problem of determining the boundary of a swept volume, some difficulties may arise. A first difficulty may occur in the process of obtaining the equation of the envelope; the locus found by the process described above may contain curves other than the envelope. For instance if the curves of the family $F = 0$ have singular points and if $\mathbf{x} = \phi(t)$ is the locus

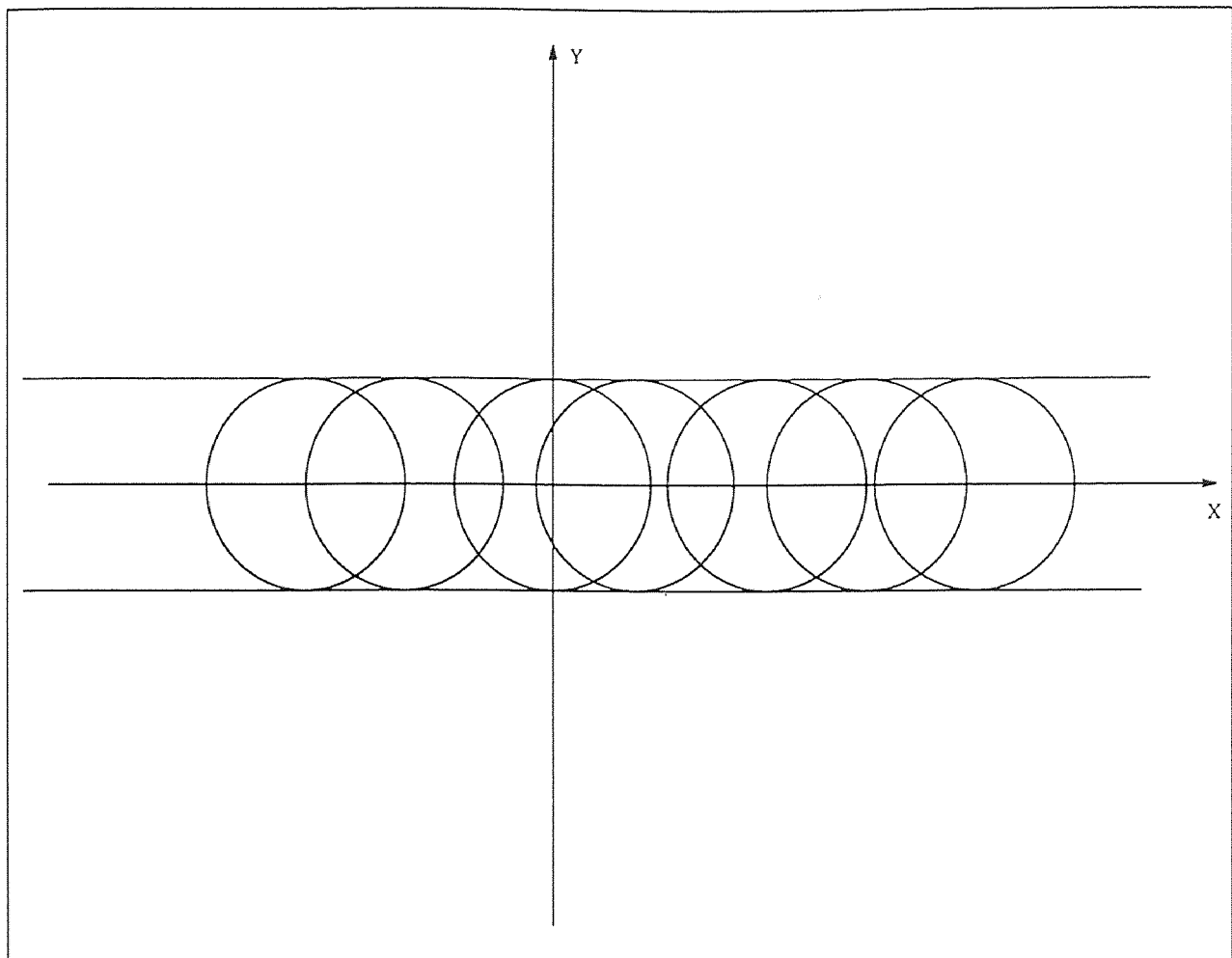


Figure 1 Envelope of a family of circles whose centers are along the x axis

of the singular points as t varies, (1) and (2) will hold, thus the rule for finding the envelope leads also to the locus of the singular points. Other extraneous factors may also be introduced in performing the elimination. We must take special care in the eliminaton process, otherwise not only may extraneous solutions be mistaken for the envelope, but the envelope may be missed completely.

Example 1.2 Consider $y - \sin tx = 0$ and $t - x^{-1} \sin^{-1} y = 0$. The families of curves are identical, and it is geometrically clear that $y = \pm 1$ is their envelope. This is precisely the result if we eliminate t from $F = 0$ and $F_t = 0$ of the first family. But if we apply the same process to the second, we will find $F_t = 1 \neq 0$, which does not vanish and hence indicates no envelope.

The above process should be checked carefully using the implicit function theorem. A second difficulty can occur when the actual object is a finite piece of an infinite object. Direct application of the envelope equation often yields points which are not on the boundary of the swept volume. This is illustrated in the following example.

Example 1.3 Consider the swept volume of the line segment $\{| y | \leq 1, x = 0\}$. under the following general 2-D motion:

$$\sigma_t \begin{bmatrix} x \\ y \end{bmatrix} = \begin{bmatrix} \xi(t) \\ \eta(t) \end{bmatrix} + \begin{bmatrix} \cos \theta(t) & -\sin \theta(t) \\ \sin \theta(t) & \cos \theta(t) \end{bmatrix} \begin{bmatrix} x_0 \\ y_0 \end{bmatrix},$$

where (x_0, y_0) describes the inital position of the points. From the sweep equation above, it is easy to derive the equation for the whole swept volume (or the family of line segments produced while sweeping); namely:

$$\frac{y - y_a(t)}{x - x_a(t)} = \frac{y_b(t) - y_a(t)}{x_b(t) - x_a(t)} = \frac{-2 \cos \theta}{2 \sin \theta} = -\cot \theta$$

where $(x_a(t), y_a(t)), (x_b(t), y_b(t))$ are the positions of the end points at time t .

$$\implies x \cos \theta + y \sin \theta - (\xi \cos \theta + \eta \sin \theta) = 0$$

$$F(x, y, t) = 0 : \quad x \cos \theta + y \sin \theta - (\xi \cos \theta + \eta \sin \theta) = 0 \quad (6)$$

$$F_t(x, y, t) = 0 : \quad \dot{\theta}[-x \sin \theta + y \cos \theta - (-\xi \sin \theta + \eta \cos \theta)] \\ -(\dot{\xi} \cos \theta + \dot{\eta} \sin \theta) = 0 \quad (7)$$

Solving for the envelope $x = x(t), y = y(t)$, we obtain

$$\begin{bmatrix} \cos \theta & \sin \theta \\ -\dot{\theta} \sin \theta & \dot{\theta} \cos \theta \end{bmatrix} \begin{bmatrix} x \\ y \end{bmatrix} = \begin{bmatrix} \cos \theta & \sin \theta \\ -\dot{\theta} \sin \theta & \dot{\theta} \cos \theta \end{bmatrix} \begin{bmatrix} \xi \\ \eta \end{bmatrix} + \begin{bmatrix} 0 \\ \dot{\xi} \cos \theta + \dot{\eta} \sin \theta \end{bmatrix}$$

Notice that

$$\det \begin{bmatrix} \cos \theta & \sin \theta \\ -\dot{\theta} \sin \theta & \dot{\theta} \cos \theta \end{bmatrix} = \dot{\theta}$$

If $\dot{\theta} \neq 0$, then:

$$\begin{bmatrix} x \\ y \end{bmatrix} = \begin{bmatrix} \xi \\ \eta \end{bmatrix} + \frac{1}{\dot{\theta}} \begin{bmatrix} \dot{\theta} \cos \theta & -\sin \theta \\ \dot{\theta} \sin \theta & \cos \theta \end{bmatrix} \begin{bmatrix} 0 \\ \dot{\xi} \cos \theta + \dot{\eta} \sin \theta \end{bmatrix}$$

$$\implies \begin{bmatrix} x \\ y \end{bmatrix} = \begin{bmatrix} \xi \\ \eta \end{bmatrix} + \frac{1}{\dot{\theta}} \begin{bmatrix} -\sin \theta(\dot{\xi} \cos \theta + \dot{\eta} \sin \theta) \\ \cos \theta(\dot{\xi} \cos \theta + \dot{\eta} \sin \theta) \end{bmatrix}$$

$$\implies \begin{bmatrix} x \\ y \end{bmatrix} = \begin{bmatrix} \xi \\ \eta \end{bmatrix} + \frac{\dot{\xi} \cos \theta + \dot{\eta} \sin \theta}{\dot{\theta}} \begin{bmatrix} -\sin \theta \\ \cos \theta \end{bmatrix}$$

When $\xi = 4t, \eta = 0$ and $\theta(t) = \pi t$, the swept volume and the envelope obtained from the above equations are shown in figures 2 and 3. One can clearly see the portion of the envelope which is not part of the swept volume boundary; this is due to the finite extent of the object undergoing the sweep, that is, the line family equation we derived is in fact the equation of a line of infinite length which contains the swept line segment.

The envelope we obtain thus is actually the envelope of the family of lines, which also contains points which are outside the line segment being swept.

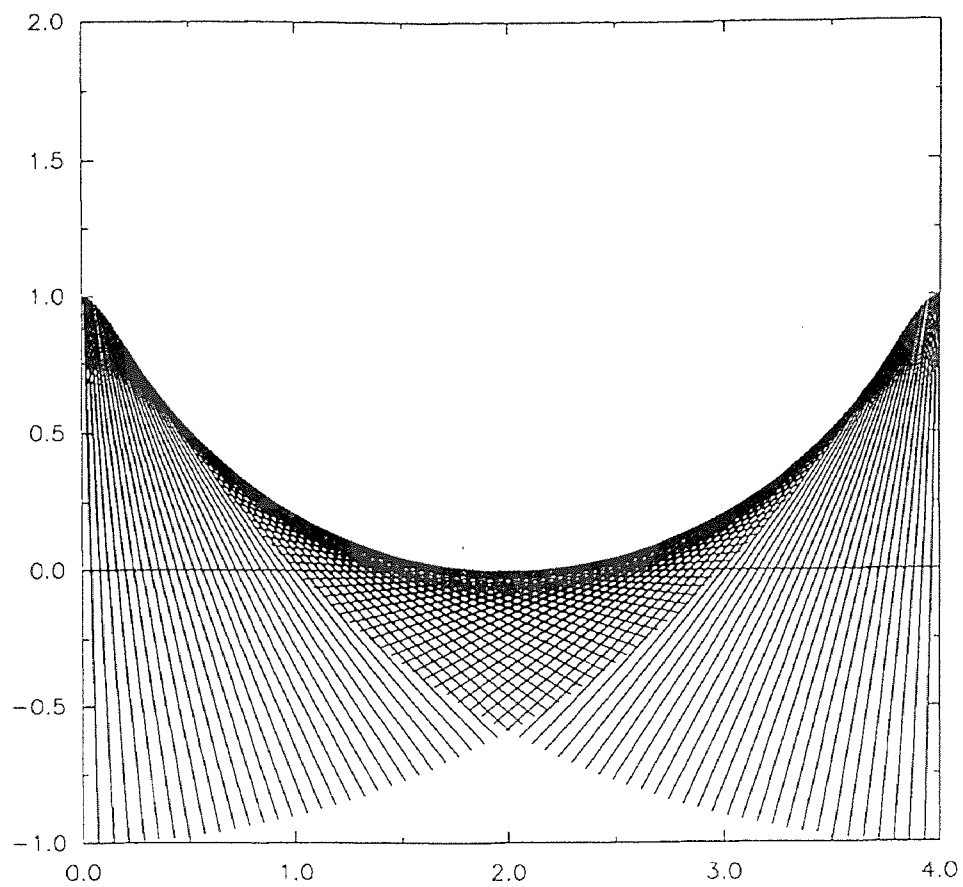


Figure 2 Swept volume of a line segment undergoing a 2-D sweep

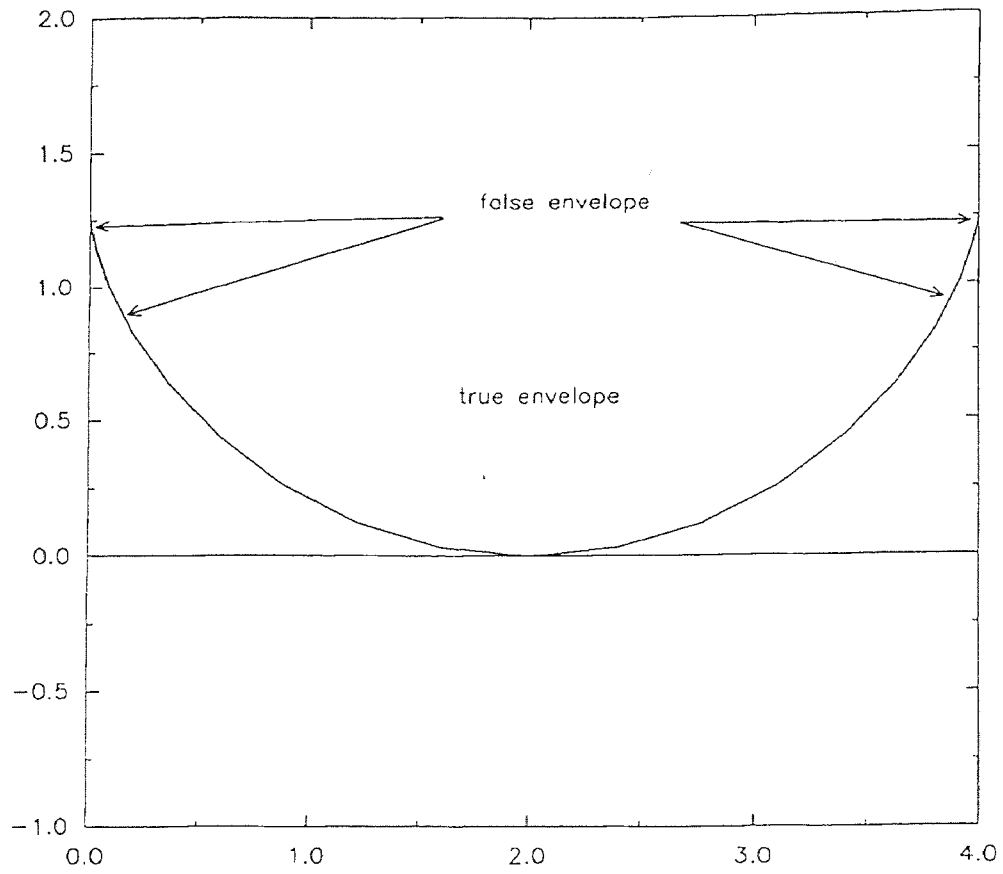


Figure 3 Envelope curve of the swept volume of a line segment

If the $\dot{\theta} = 0$, then the equation for the envelope is undefined since we are dividing by zero. Nevertheless, useful information can still be obtained from the equations.

$$\dot{\theta} = 0 \implies$$

$$F(x, y, t) = 0 : \quad x \cos \theta + y \sin \theta - (\xi \cos \theta + \eta \sin \theta) = 0$$

$$F_t(x, y, t) = 0 : \quad \dot{\xi} \cos \theta + \dot{\eta} \sin \theta = 0$$

This system of equations may not have a solution at all or will have infinitely many solutions if $\dot{\xi} \cos \theta + \dot{\eta} \sin \theta = 0$.

A third difficulty lies in the fact that in order to obtain the envelope, one usually needs to solve a system of nonlinear equations using numerical methods, which may require large amount of CPU time. In this case, one may put some restrictions on the shape of the object or on the type of sweep in order to simplify the problem (e.g. [15]).

In one of the most recent and successful efforts using envelope theory, Sambandan[20] took an indirect approach to solving the envelope equations. He developed an envelope criterion which basically is equivalent to our candidate boundary point selection criterion. On the edge across which there is a discontinuity of surface normals, he adjusted the definition of the normal there in order to apply the envelope criterion. Due to the difficulty of evaluating the velocity at given points, he used another alternative which requires the computation of the instantaneous rotation center of the motion at each time instant and then found the points on the boundary of the object whose distances from the instantaneous rotation center are local extrema. This computational work, as we shall see in the following chapters, is necessary if the problem is considered in the context of sweep differential equations and sweep vector fields.

In addition, Sambandan's approach has other features which we shall try to improve on using our method; They are:

- He developed a local higher order derivative criterion to reduce the number of candidate boundary points. It required the computation of higher order derivatives. These derivatives were checked to see if they were zero, and if they were not zero, their sign had to be determined. This may cause numerical difficulties and may not be completely reliable; in particular, the criterion will not be applicable if all of the derivatives vanish, and it may produce incorrect results when some of the derivatives are very close to zero in value. This may explain why he did not implement this criterion in his programs.
- The trimming procedure developed by Sambandan can not deal with the case when the swept volume has "holes", i. e. when the boundary of a planar swept volume has more than one connected component.
- Sambandan's trimming procedure apparently cannot be extended to 3-D swept volumes.

Recently, Blackmore and Leu [2], [3], [4], [5] have developed a very general method for analyzing and representing swept volume which they called the sweep differential equation approach. Their approach has several points in common with the envelope method; in fact, it can be shown that the envelope method can be derived from the sweep differential equation approach. The algorithm for computing planar swept volume which we develop in this thesis is directly based on the approach of Blackmore and Leu. It will be shown that this approach leads to several theoretical and computational improvements of existing methods for characterizing and illustrating swept volumes.

The organization of this paper is as follow: In chapter 2, we introduce some basic notations and definitions, as well as some basic theorems of the sweep differential

equation approach which will be used extensively in the succeeding chapters. The sweep flow method, including our candidate boundary points selection criterion and global trimming procedure are developed in chapter 3. In chapter 4, we describe the implementation of the prototype software in the 2-D case which is based upon the theory proposed in chapter 4. Some examples are also given to illustrate the utility of our procedure. In chapter 5, we briefly discuss the extension of the sweep flow method to the 3-D case. In chapter 6, we make some relevant observations and remarks concerning the contents of this thesis and possible future research work.

CHAPTER 2
THEORETICAL PRELIMINARIES

In this chapter, we will introduce some notations and definitions, as well as some basic theorems which will be used rather extensively in the sequel. For more details, one can refer to [2] and [3]. The real numbers will be represented by \mathbf{R} . Let \mathbf{R}^n denote Euclidean n -space consisting of n -tuples of real numbers $\mathbf{x} = (x_1, x_2, \dots, x_n)$ with the usual inner product $\langle \cdot, \cdot \rangle$ and norm $\|\cdot\|$ defined by

$$\langle \mathbf{x}, \mathbf{y} \rangle = \sum_{k=1}^n x_k y_k \text{ and } \|\mathbf{x}\| = \langle \mathbf{x}, \mathbf{x} \rangle^{1/2}$$

The members of \mathbf{R}^n are often called n -vectors.

The Euclidean group $\mathbf{E}(n)$ is composed of all mappings $\mathbf{R}^n \rightarrow \mathbf{R}^n$ of the form $\mathbf{x} \rightarrow \xi + A\mathbf{x}$, where $\xi \in \mathbf{R}^n$, and $A \in \mathbf{SO}(n)$; here $\mathbf{SO}(n)$ is the special orthogonal group consisting of all real, $n \times n$ orthogonal matrices A with $\det A = 1$.

Definition 2.1 A *sweep* σ is a continuous mapping of the unit interval $[0, 1]$ into the group $\mathbf{E}(n)$ of rigid motions in the \mathbf{R}^n , which is initially the identity. Let σ_t denote the value of sweep at time $t, t \in [0, 1]$, then we can write the sweep equation:

$$\sigma_t(\mathbf{x}) = \xi(t) + A(t)\mathbf{x}$$

where $\xi : [0, 1] \rightarrow \mathbf{R}^n$ and $A : [0, 1] \rightarrow \mathbf{SO}(n)$ are continuous and satisfy $\xi(0) = 0$ and $A(0) = I$. Here the use of the unit time interval $[0, 1]$ in our definition involves no loss of generality, since the parameter can always be scaled to range between 0 and 1.

Definition 2.2 Let σ be a sweep and M be an object in \mathbf{R}^n . The *swept volume* of M generated by σ is the region:

$$S_\sigma(M) = \{\sigma_t(\mathbf{x}) : \mathbf{x} \in M, t \in [0, 1]\}$$

The sets $\sigma_t(M) = \{\sigma_t(\mathbf{x}) : \mathbf{x} \in M\}$ are the t -sections of M generated by the sweep σ and $\sigma(\mathbf{x}) = \{\sigma_t(\mathbf{x}) : t \in [0, 1]\}$ is the σ -trajectory of \mathbf{x} .

Definition 2.3 Let $\sigma_t = \xi(t) + A(t)\mathbf{x}$ be a smooth sweep (i. e. a sweep for which ξ and A have continuous derivatives of all orders). The *sweep vector field(SVF)* corresponding to σ is the smooth vector field X_σ defined by

$$X_\sigma(\mathbf{x}, t) = \dot{\xi}(t) + \dot{A}(t)A^T(t)(\mathbf{x} - \xi(t))$$

We call the differential equation

$$\dot{\mathbf{x}} = \frac{d\mathbf{x}}{dt} = X_\sigma(\mathbf{x}, t) \equiv \dot{\xi}(t) + \dot{A}(t)A^T(t)(\mathbf{x} - \xi(t))$$

associated with this vector field the *sweep differential equation (SDE)* of σ . Here the dot denotes differentiation with respect to t and the superscript denotes the transpose. It should be noted that $\dot{A}(t)A^T(t) \in \mathfrak{o}(n)$ for $t \in [0, 1]$, where $\mathfrak{o}(n) = \{B_{n \times n} : B + B^T = 0\}$ is the set of real skew-symmetric matrices.

Definition 2.4 A smooth sweep σ is *autonomous* if its sweep differential equation

$$\frac{d\mathbf{x}}{dt} = X_\sigma(\mathbf{x}, t) \equiv \dot{\xi}(t) + \dot{A}(t)A^T(t)(\mathbf{x} - \xi(t))$$

is an autonomous differential equation.

A necessary and sufficient condition for σ to be autonomous is that $\frac{\partial X_\sigma}{\partial t} = 0$; that is, the sweep vector field X_σ is independent of time variable t . It can be shown (see [2]) that the SDE of an autonomous sweep has the form

$$\dot{\mathbf{x}} = B\mathbf{x} + c$$

Definition 2.5 The *extended sweep differential equation (ESDE)* of σ is defined as:

$$\begin{aligned} \frac{d\mathbf{x}}{ds} &= X_\sigma(\mathbf{x}, t) \\ \frac{dt}{ds} &= 1 \end{aligned}$$

which can be written in the more concise form

$$\frac{du}{ds} = X_\sigma^*(u)$$

where $u = (\mathbf{x}, t)$ and $X_\sigma^* = (X_\sigma(u), 1)$. X_σ^* is called the *extended sweep vector field (ESVF)* of σ .

Definition 2.6 If $\sigma : [0, 1] \rightarrow \mathbf{E}(n)$ is a sweep defined by $\sigma_t(\mathbf{x}) = \xi(t) + A(t)\mathbf{x}$, the mapping $\sigma^* : [0, 1] \rightarrow \mathbf{E}(n) \times \mathbf{R}$ defined by $\sigma^*(\mathbf{x}, t) = (\sigma(\mathbf{x}), s + t)$ is its *extended sweep*. The *extended swept volume* of the object M under the sweep σ is

$$S_\sigma^*(M) = \cup\{\sigma_s^*(M) : s \in [0, 1]\}$$

Where M is identified with $M \times 0 = \{(\mathbf{x}, t) : \mathbf{x} \in M, t = 0\}$ in $\mathbf{R}^n \times \mathbf{R}$.

The connection between the swept volume and extended swept volume is given by following lemma:

Lemma 2.1

$$S_\sigma(M) = \Pi(S_\sigma^*(M))$$

Where the projection $\Pi : \mathbf{R}^{n+1} \rightarrow \mathbf{R}^n$ is defined to be the natural projection onto the first n coordinates; namely, $\Pi(\mathbf{x}, t) = \mathbf{x}$.

Definition 2.7 Let M be a codimension 1 submanifold of \mathbf{R}^n . A sweep σ is of *type I with respect to (wrt) M* if the mapping

$$\Sigma : M \times [0, 1] \rightarrow S_\sigma(M) \subset \mathbf{R}^n$$

defined by

$$\Sigma(\mathbf{x}, t) = \sigma_t(\mathbf{x})$$

satisfies the following properties:

- If $\mathbf{x} \in \text{int}(M)$, then $\sigma_t(\mathbf{x}) = \Sigma(\mathbf{x}, t) \in \text{Int}(S_\sigma(M))$,

- If $\mathbf{x} \in \partial M$, then $\sigma_t(\mathbf{x}) \in Fr(S_\sigma(M))$ for every $t \in (0, 1)$.

Here Int denotes the (topological) interior and Fr the frontier or boundary of a set. Otherwise, we say that σ is of *type II wrt M* .

Note that $Int(M)$ and ∂M refer to subsets of M defined in terms of its manifold structure. $Int(S_\sigma(M))$ and $Fr(S_\sigma(M))$ refer to the relative topology of $S_\sigma(M)$ as a subset of \mathbf{R}^n (see [7]). In particular, $\mathbf{x} \in Int(S_\sigma(M))$ if there exists an open neighborhood U of \mathbf{x} in \mathbf{R}^n such that $U \subset S_\sigma(M)$, and $\mathbf{x} \in Fr(S_\sigma(M))$, the frontier (or boundary) of $S_\sigma(M)$, if every open neighborhood of \mathbf{x} in \mathbf{R}^n contains points of both $S_\sigma(M)$ and its complement.

Definition 2.8 A smooth sweep σ is *regular with respect to (wrt) M* if the smooth mapping Σ is a homeomorphism of $M \times [0, 1]$ onto $S_\sigma(M)$ and is a smooth diffeomorphism on the interior of $M \times [0, 1]$. We say that σ is *regular periodic wrt M* when $\sigma_1(M) = M$ and Σ induces a homeomorphism from $M \times S^1$ to $S_\sigma(M)$ which is a smooth diffeomorphism on the interior of $M \times S^1$, where S^1 is the unit circle. If σ is not regular or regular periodic, it is *singular wrt M* .

Theorem 2.1 *Let M be as defined above and σ be a smooth map. Then σ is of type I wrt M if σ is regular or regular periodic wrt M .*

Theorem 2.2 *Let σ be a smooth sweep in \mathbf{R}^n and M be a codimension 1 submanifold as described above. Suppose that the sweep vector field $X_\sigma(\mathbf{x}, t)$ is nonvanishing on $\sigma_t(M)$ and is transverse (not tangent) to the interior of $\sigma_t(M)$ for every $0 \leq t \leq 1$. In addition, suppose that $S_\sigma(M)$ never intersects itself, or more precisely, the natural projection Π of the extended swept volume onto the swept volume is injective (one-to-one). Then σ is regular wrt M (and therefore of type I wrt M).*

The proofs of the above theorems can be found in [2].

The nontangency hypothesis of this theorem can be readily checked as follows:

Define

$$\begin{aligned} T(\mathbf{x}, t) &= \langle X_\sigma(\sigma_t(\mathbf{x}), t), N_t(\sigma_t(\mathbf{x})) \rangle \\ &= \langle X_\sigma(\sigma_t(\mathbf{x}), t), A(t)N_0(\mathbf{x}) \rangle \end{aligned} \quad (8)$$

where the unit normal family $N_t : 0 \leq t \leq 1$ is a collection of unit vector fields such that N_t is normal to $\sigma_t(M)$ at every point t of the interval $[0, 1]$. It is easy to see that the nontangency condition is tantamount to the requirement that T be nonzero on $Int(M) \times [0, 1]$.

Definition 2.9 The *tangency condition* refers to the following equation:

$$T(\mathbf{x}, t) = 0 \quad (9)$$

CHAPTER 3

THE THEORY OF THE SWEEP FLOW APPROACH

3.1 The General Evaluation Procedure

In this chapter, we will introduce the basic theory of the sweep flow approach to the swept volume problem, which can be stated as follows:

Given an object M and smooth rigid sweep σ , and the sweep time interval $[0, 1]$, we want to obtain the boundary representation of the swept volume generated by the object M undergoing the sweep σ during the time interval $[0, 1]$.

The assumption of unit time interval $[0, 1]$ here will result in no loss of generality, since any time interval can be scaled to range between 0 and 1.

Generally speaking, our evaluation scheme is similar to the “local generation and global trimming” category as in [20] etc., however, several improvements can be made in comparison to the existing approaches.

Our general evaluation process can be outlined as follows:

Input:

Solid object M

Sweep differential equation:

$$\dot{\mathbf{x}} = X_\sigma = \dot{\xi} + \dot{A}A^T(\mathbf{x} - \xi)$$

The unit time interval $[0, 1]$.

Local generation and trimming:

Divide the time interval $[0, 1]$ into a finite number of intermediate instants. At each time instant, generate the candidate boundary patches which satisfy the cri-

terion we will describe in the sequel. We will use the local trimming procedure to immediately trim out those candidate boundary patches which belong to the interior of the swept volume.

Global trimming:

Trim those candidate boundary patches which are in fact members of the interior of the swept volume and thus produce the boundary patches of the swept volume. The global trimming will include two steps: *initial global trimming* and *secondary global trimming*.

Boundary forming:

Connect the boundary patches properly to form the piecewise approximation of the boundary of the swept volume.

Output:

Boundary representation of the swept volume

The trimming process is necessarily global since the boundary patch of swept volume at some time t_i may belong to the interior of the swept volume at t_j , where t_j may be greater than t_i or less than t_i . This is illustrated in figure 4. In fact, effective implementation of the trimming procedure is the most challenging part of our research.

3.2 The Selection of Candidate Boundary Points

It has been shown in Weld & Leu[25] (see also [24]) that for any given sweep σ , if the object M is a compact, n -dimensional submanifold of \mathbf{R}^n possessing a piecewise

smooth boundary ∂M , the swept volume of the object M is given by

$$S_\sigma(M) = M \cup S_\sigma(\partial M)$$

and this will reduce to

$$S_\sigma(M) = S_\sigma(\partial M)$$

if $M \cap \sigma_t(M) = \phi$ for $t \in (0, 1)$. This means that the swept volume of the n -dimensional manifold M is actually determined by the swept volume of ∂M , which is of codimension 1 in the object M . In what follows, we shall assume that the object M is a compact, n -dimensional submanifold of \mathbf{R}^n with a piecewise smooth boundary.

Blackmore & Leu [5] study the linear, circular and helical sweeps in \mathbf{R}^3 which constitute one special class of sweep which they call autonomous sweeps, and use a technique they call the boundary flow method (**BFM**), which is based on the sweep differential equation approach, to compute the swept volume.

Our approach, which is also based on the sweep differential equations and sweep vector fields can be viewed as the natural extension of the **BFM** to general sweeps. At any time t , the boundary of the object M can be partitioned into three sets:

$$\partial M(t) = \partial_- M(t) \cup \partial_0 M(t) \cup \partial_+ M(t)$$

Where $\partial_+ M(t)$ is called the *instantaneous ingress point* set, $\partial_0 M(t)$ is the set of *instantaneous grazing points* and $\partial_- M(t)$ is the *instantaneous egress point* set. A point $\mathbf{x} \in \partial M$ is an instantaneous ingress point at time t if the sweep vector at \mathbf{x} at time t is directed into the interior of M , it is an instantaneous egress point if the sweep vector at \mathbf{x} at time t is directed out of the interior of M ; otherwise it is a grazing point. From this definition, it is straightforward to decide if a point $\mathbf{x} \in \partial M$ is an ingress, egress or grazing point at time t . This may be done as follows: If \mathbf{x} belongs to a smooth portion of ∂M , and $N(\mathbf{x}, t)$ is the normal vector to ∂M at \mathbf{x} pointing into the interior of the object M , we set $T(\mathbf{x}, t) = \langle X_\sigma(\mathbf{x}, t), N(\mathbf{x}, t) \rangle$. Then \mathbf{x} is an

instantaneous ingress point, egress points or grazing point at time t according as the sign of $T(\mathbf{x}, t)$ is positive, negative or zero, respectively. If \mathbf{x} belongs to the edge of two contiguous smooth portions of ∂M , then it can be assumed to have two normal vectors—the normal vectors of the abutting smooth surfaces, say $N_1(\mathbf{x}, t), N_2(\mathbf{x}, t)$. It is an instantaneous ingress point, egress points or grazing point at time t according as the signs of $T_1(\mathbf{x}, t)$ and $T_2(\mathbf{x}, t)$ are both positive, both negative or otherwise, respectively.

In general, a point \mathbf{x} can belong to k surfaces which abut each other at \mathbf{x} (e. g. the vertex of a cube in 3-D space), then we can assign k normal vectors to it, say $N_1(\mathbf{x}, t), \dots, N_k(\mathbf{x}, t)$, and it is an instantaneous ingress point, egress points or grazing point at time t according as the signs of $T_1(\mathbf{x}, t), \dots, T_k(\mathbf{x}, t)$ are all positive, all negative or otherwise, respectively. A point \mathbf{x} can also belong to a surface; but have a 1-parameter family of normal vectors associated with it (e. g. the vertex of a cone in 3-D space). The sign of the family $T_\alpha(\mathbf{x}, t)$ can then be used to determine ingress, egress and grazing points in the obvious way. Figure 5 is a 2-D example of boundary partition.

Notice that the definition for a grazing point on smooth portions of ∂M coincides with the tangency condition of chapter 2, that is:

$$\begin{aligned} T(\mathbf{x}, t) &= \langle X_\sigma(\sigma_t(\mathbf{x}), t), N_t(\sigma_t(\mathbf{x})) \rangle \\ &= \langle X_\sigma(\sigma_t(\mathbf{x}), t), A(t)N_0(\mathbf{x}) \rangle \\ &= 0 \end{aligned} \tag{1}$$

The relationship between grazing points and envelope points is given by the following theorem:

Theorem 3.1 *Given an object M undergoing a smooth sweep σ , the grazing points of the smooth portion of $\partial M(t)$ (The points that satisfy the tangency condition $T(\mathbf{x}, t) =$*

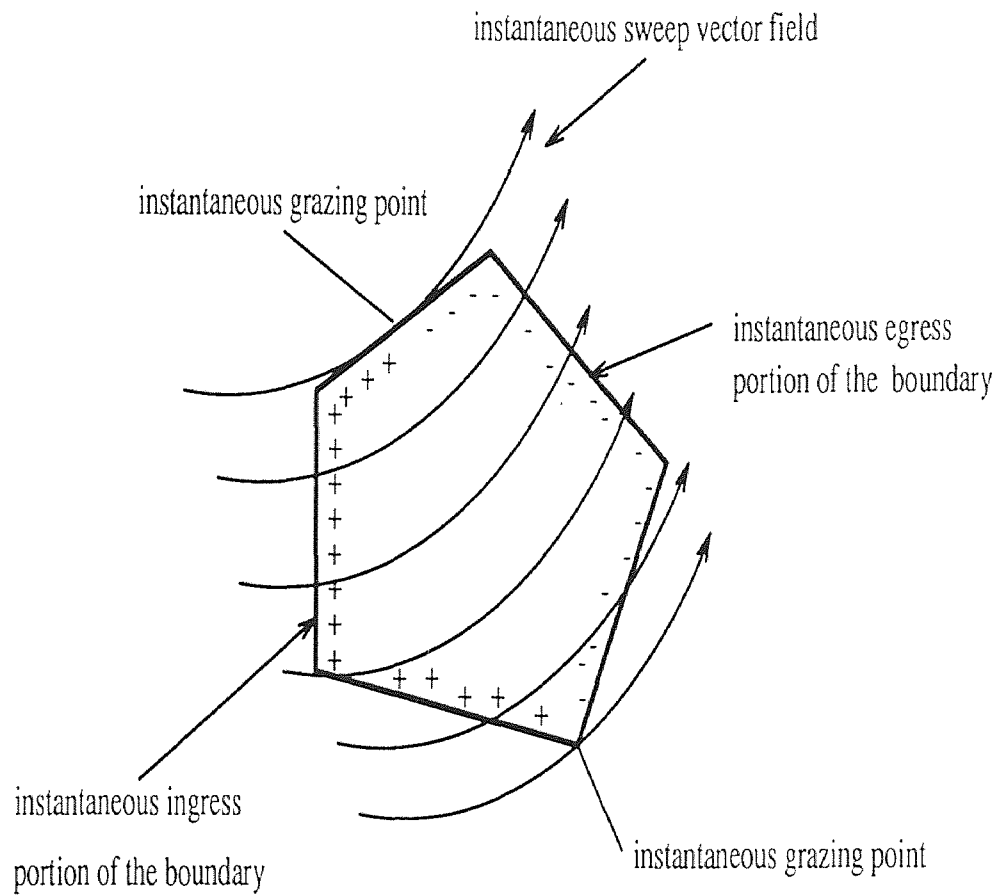


Figure 5 Illustration of partition of the boundary

$0, \mathbf{x} \in \partial M$) as t ranges over $[0, 1]$ are the envelope points of the family $\sigma_t(\partial M), t \in [0, 1]$.

Proof. Let \mathbf{x}^0 belong to the smooth portion of ∂M . Then by a standard result of differential topology(see [14]), there exists an open neighborhood U of \mathbf{x}^0 in \mathbb{R}^n and a smooth function $f : U \rightarrow \mathbb{R}^n$ such that

$$W = U \cap \partial M = \{\mathbf{x}^0 \in U : f(\mathbf{x}^0) = 0\}$$

It is not difficult to see that the family $\{\sigma_t(W) : 0 \leq t \leq 1\}$ is characterized by

$$F(\mathbf{x}, t) = 0$$

where

$$F(\mathbf{x}, t) = f(\sigma_t^{-1}(\mathbf{x})) = f(A^T(t)(\mathbf{x} - \xi(t)))$$

The envelope points of the family $\{\sigma_t(W)\}$ are obtained from the equations

$$F(\mathbf{x}, t) = 0$$

$$F_t(\mathbf{x}, t) = 0$$

Using the chain rule, we compute that

$$\begin{aligned} F_t(\mathbf{x}, t) &= \frac{\partial}{\partial t} f(A^T(t)(\mathbf{x} - \xi(t))) \\ &= \left\langle \nabla f(A^T(t)(\mathbf{x} - \xi(t))), \dot{A}^T(t)(\mathbf{x} - \xi(t)) - A^T \dot{\xi}(t) \right\rangle \\ &= \left\langle \nabla f(A^T(t)(\mathbf{x} - \xi(t))), A^T[A \dot{A}^T(\mathbf{x} - \xi) - \dot{\xi}] \right\rangle \\ &= \left\langle \nabla f(A^T(t)(\mathbf{x} - \xi(t))), A^T[-\dot{A}A^T(\mathbf{x} - \xi) - \dot{\xi}] \right\rangle \end{aligned}$$

since $AA^T = I$ implies that $\dot{A}A^T + A\dot{A}^T = 0$. Hence

$$F_t(\mathbf{x}, t) = - \left\langle \nabla f(A^T(t)(\mathbf{x} - \xi(t))), A^T X_\sigma(\mathbf{x}, t) \right\rangle,$$

from which we conclude that

$$\begin{aligned} F_t(\sigma_t(\mathbf{x}^0), t) &= - \left\langle \nabla f(\mathbf{x}^0), A^T X_\sigma(\sigma_t(\mathbf{x}^0), t) \right\rangle \\ &= - \left\langle X_\sigma(\sigma_t(\mathbf{x}^0), t), A(t) \nabla f(\mathbf{x}^0) \right\rangle \end{aligned}$$

But, since $\nabla f(\mathbf{x}^0)$ is normal to W ,

$$\nabla f(\mathbf{x}^0) = -KN(\mathbf{x}^0),$$

where N defines the normal family and K is a positive nonzero constant. Hence

$$F_t(\sigma_t(\mathbf{x}^0, t)) = KT(\mathbf{x}^0, t) \quad (2)$$

and therefore we see that envelope points coincide with points satisfying $T = 0$. This completes the proof.

Theorem 3.2 *Let σ be a given smooth sweep in \mathbf{R}^n and M an object. Then the boundary of the swept volume of M satisfies the following formula:*

$$\partial S_\sigma(M) \subseteq \left\{ \bigcup_{t=0}^1 \partial_0 M(t) \right\} \cup \partial_+ M(0) \cup \partial_- M(1) \quad (3)$$

where $t \in [0, 1]$

Here we use \subseteq instead of $=$ because of the global nature of the sweep process which we mentioned before.

Proof. We first note that by the properties of the object M there exists a piecewise smooth function $f : \mathbf{R}^n \rightarrow \mathbf{R}$ such that f is negative in the interior of M , f is positive on the exterior of M and f vanishes on the boundary of M . This implies that the function $F : \mathbf{R}^n \times [0, 1] \rightarrow \mathbf{R}$ defined by

$$F(\mathbf{x}, t) = f(A^T(t)(\mathbf{x} - \xi(t)))$$

characterizes the t -sections of the swept volume of M as follows:

$$\partial M(t) = \{\mathbf{x} \in \mathbf{R}^n : F(\mathbf{x}, t) = 0\}$$

$$\text{int}M(t) = \{\mathbf{x} \in \mathbf{R}^n : F(\mathbf{x}, t) < 0\}$$

$$\text{ext}M(t) = \mathbf{R}^n \setminus M(t) = \{\mathbf{x} \in \mathbf{R}^n : F(\mathbf{x}, t) > 0\}$$

Let $\mathbf{x}^0 \in \partial M(t)$ for some $0 \leq t \leq 1$. It is easy to see that $\partial_+ M(0) \cup \partial_- M(1)$ may contain boundary points of the swept volume, so we shall assume that

$$\mathbf{x}^0 \notin \partial_+ M(0) \cup \partial_- M(1)$$

Clearly the proof is complete if we show that $\mathbf{x}^0 \in \partial_0 M(t)$ for some $0 \leq t \leq 1$. This will be done by contradiction.

Suppose, on the contrary, that $\mathbf{x}^0 \in \partial_+ M(t_0)$ for some $0 < t_0 \leq 1$ or $\mathbf{x}^0 \in \partial_- M(t_0)$ for some $0 \leq t_0 < 1$. We shall only show that $\mathbf{x}^0 \in \partial_+ M(t_0)$ leads to a contradiction, since the proof of the contradictory nature of the second supposed alternative is analogous. The definition of an ingress point implies that there is an $0 \leq \epsilon < t_0$ such that $F(\mathbf{x}^0, t)$ is a strictly increasing function of t on $(t_0 - \epsilon, t_0 + \epsilon)$. As $F(\mathbf{x}^0, t_0) = 0$, we infer that $F(\mathbf{x}^0, t_0 - \epsilon) < 0$, which implies that \mathbf{x}^0 belongs to the interior of $M(t_0 - \epsilon)$. Hence there exist an open neighborhood U of \mathbf{x}^0 such that

$$U \subseteq M(t_0 - \epsilon) = \sigma_{t_0 - \epsilon}(M) \subseteq S_\sigma(M)$$

This contradicts our basic premise that $\mathbf{x}^0 \in \partial S_\sigma(M)$, and this concludes the proof.

Corollary 3.1 *Let σ be a linear, circular or helical sweep in \mathbf{R}^3 such that X_σ has no zeros in the object M and $S_\sigma(\partial M)$ has no self-intersections. Then the boundary of the swept volume of M is given by the formula*

$$\partial S_\sigma(M) = S_\sigma(\partial_0 M(0)) \cup \partial_- M \cup \partial_+ M(1)$$

Proof. From the above theorem, the proof of this corollary is straightforward. Since the linear, circular or helical sweeps in \mathbf{R}^3 have been shown in [4] to constitute the class of autonomous sweeps for which the sweep vector field is independent of time t , we see that

$$\begin{aligned} \mathbf{x} \in \partial_0 M(0) &\implies \sigma_t(\mathbf{x}) \in \sigma_t(\partial_0 M(0)) = \partial_0 M(t) \\ &\implies \bigcup_{t=0}^1 \partial_0 M(t) = S_\sigma(\partial_0 M(0)) \end{aligned}$$

As there are no intersections, the global trimming is unnecessary in this case, and we can use $=$ instead of \subseteq in the formula (12). Thus the proof is complete.

3.3 The Global Trimming Procedure for the Candidate Boundary Points

The candidate boundary patch selection process results in a set of candidate boundary patches which are guaranteed to contain the boundary of the swept volume.

In order to trim those candidate boundary patches or the portions of candidate patches which belong to the interior of the swept volume, we need an efficient way of determining whether or not a patch belongs to the interior of some t -section of the swept volume.

The global trimming procedure can also be viewed from the extended sweep point of view. The extended swept volume, which is imbedded in \mathbf{R}^{n+1} spacetime, is much better behaved than the swept volume in \mathbf{R}^n since it has no self-intersections. Figure 6 is an example of an extended swept volume of a 2-D sweep. By intuition, one can immediately see that a candidate boundary point \mathbf{x}_0 should not be kept if the line $\mathbf{x} = \mathbf{x}_0$ intersects the interior of the extended swept volume. If this line does not intersect the interior of the extended swept volume, but intersects the boundary at more than one point, it may not be a boundary point; such cases will be handled by a secondary global trimming procedure.

Although it is very difficult to implement a general global trimming procedure for \mathbf{R}^n , it is possible to construct efficient algorithms for specific dimensions (like the algorithm we will describe in the implementation chapter for 2-D space). In addition, we shall see that there are local trimming techniques which can immediately be applied to certain grazing points.

Implementation of a global trimming procedure is quite problematical, but a theoretical characterization is not at all difficult as shown by the following result.

Theorem 3.3 (*Global Trimming Criterion*) *Let σ be a smooth sweep of the form $\sigma_t(\mathbf{x}) = \xi(t) + A(t)\mathbf{x}$ and let M be an object which can be characterized by a con-*

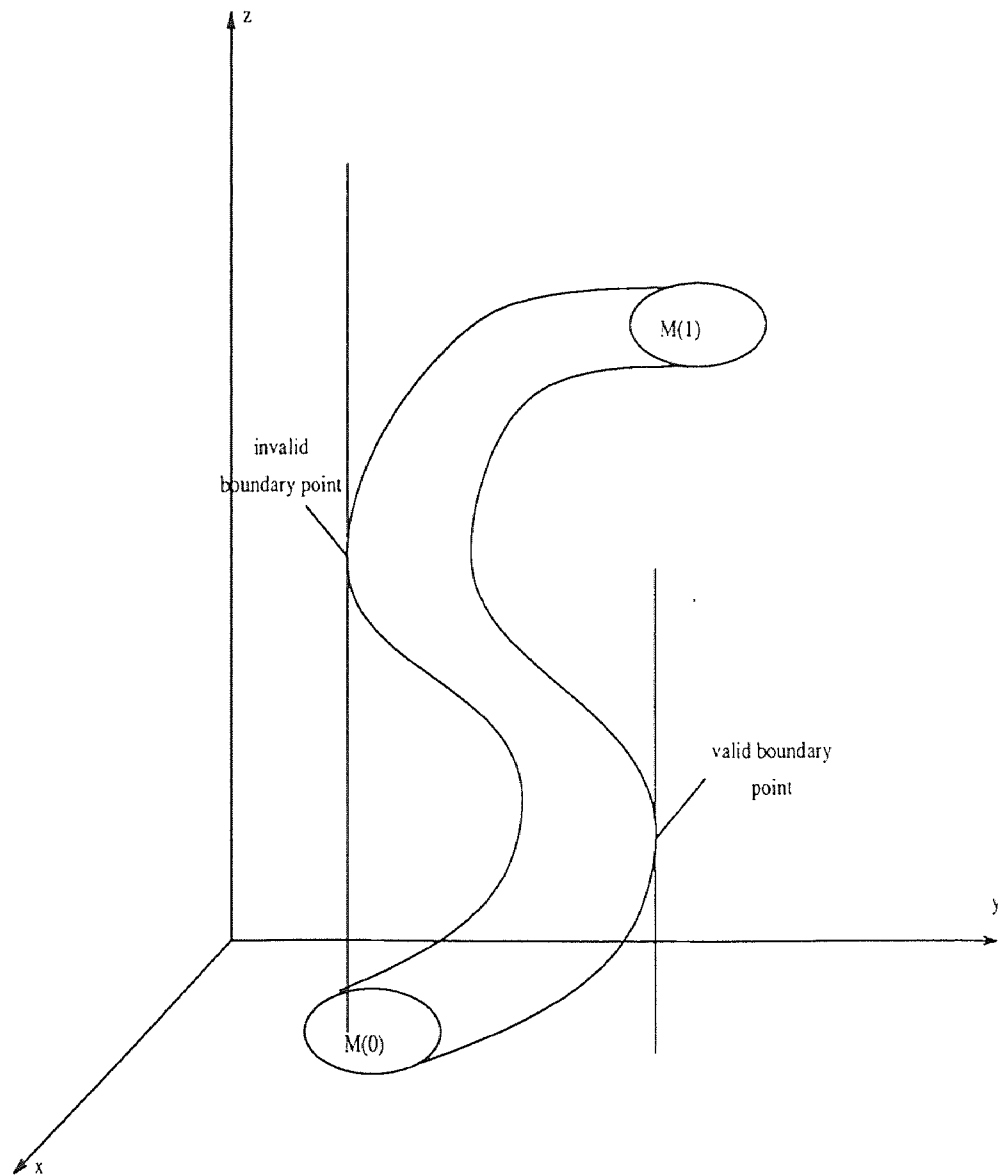


Figure 6 Global trimming procedure from extended sweep point of view

tinuous, piecewise smooth function $f : \mathbf{R}^n \rightarrow \mathbf{R}$ such that $\text{int}M = \{\mathbf{x} \in \mathbf{R}^n : f(\mathbf{x}) < 0\}$, $\partial M = \{\mathbf{x} \in \mathbf{R}^n : f(\mathbf{x}) = 0\}$ and $\text{ext}M = \{\mathbf{x} \in \mathbf{R}^n : f(\mathbf{x}) > 0\}$. Set $F(\mathbf{x}, t) = f(A^T(t)(\mathbf{x} - \xi(t)))$. Then $\mathbf{x} \in (\bigcup_{t=0}^1 \partial_0 M(t)) \cup \partial_+ M(0) \cup \partial_- M(1)$ is a point of $\partial S_\sigma(M)$ iff \mathbf{x} satisfies following conditions:

$$(1) F(\mathbf{x}, t) \geq 0 \quad \forall t \in [0, 1]$$

(2) If \mathbf{x} satisfies (1) and $F(\mathbf{x}, t_i) = 0$ for more than one $t_i \in [0, 1]$ then it should also satisfy following condition: \forall nbd U of \mathbf{x} , there exists $\mathbf{y} \in U$ such that $F(\mathbf{y}, t) > 0 \quad \forall t \in [0, 1]$

Proof. The proof of this theorem is quite straightforward. From Theorem 3.2 as we have already proven, if σ is a given smooth sweep in \mathbf{R}^n and M an object, then the boundary of the swept volume of M satisfies the following formula:

$$\partial S_\sigma(M) \subseteq \left\{ \bigcup_{t=0}^1 \partial_0 M(t) \right\} \cup \partial_+ M(0) \cup \partial_- M(1)$$

Also we notice that the function $F : \mathbf{R}^n \times [0, 1] \rightarrow \mathbf{R}$ defined by $F(\mathbf{x}, t) = f(A^T(t)(\mathbf{x} - \xi(t)))$ characterizes the t -sections of the swept volume of M as follows:

$$\partial M(t) = \{\mathbf{x} \in \mathbf{R}^n : F(\mathbf{x}, t) = 0\}$$

$$\text{int}M(t) = \{\mathbf{x} \in \mathbf{R}^n : F(\mathbf{x}, t) < 0\}$$

$$\text{ext}M(t) = \{\mathbf{x} \in \mathbf{R}^n : F(\mathbf{x}, t) > 0\}$$

$\forall \mathbf{x} \in \{\bigcup_{t=0}^1 \partial_0 M(t)\} \cup \partial_+ M(0) \cup \partial_- M(1)$, if \mathbf{x} also satisfies $F(\mathbf{x}, t) \geq 0, \forall t \in [0, 1]$, \mathbf{x} does not belong to the interior of any t -section of the swept volume, and so is a point of $\partial S_\sigma(M)$ except possibly for singular cases (one of which we illustrate using a 2-D example in Figure 7). From Figure 7, we can see that even though \mathbf{x} does not belong to the interior of any t -section of the swept volume which means that it satisfies condition (1), it still belongs to the interior of the swept volume and needs to be trimmed. We notice that \mathbf{x} satisfies $F(\mathbf{x}, t_i) = 0$ for more than one $t_i \in [0, 1]$.

In these cases, we need to add condition (2) which means that no neighborhood of \mathbf{x} is completely contained in the swept volume of M because it contains a point \mathbf{y} which is in the complement of every t -section of M . Thus the proof is complete.

Definition 3.1 Trimming those candidate boundary points which do not satisfy the condition (1) is called *initial global trimming*. *Secondary global trimming* is the elimination of those candidate boundary points which satisfy (1) but not (2).

As a practical corollary, we have the following result:

Theorem 3.4 (*Local Trimming Procedure*) Let σ be a given smooth sweep in \mathbf{R}^n , and M the object. At time t , suppose \mathbf{x}_0 belongs to the smooth portion of $\partial M(t)$ and is a grazing point. Then \mathbf{x}_0 is not a valid boundary point if $T(\mathbf{x}_0, t - \Delta t) > 0$ or $T(\mathbf{x}_0, t + \Delta t) < 0$ for positive and arbitrarily small Δt .

Proof. We will prove only the case $T(\mathbf{x}_0, t - \Delta t) > 0$, since the proof of the second case is analogous.

Let $F(\mathbf{x}, t)$ describe the object at time t with $F(\mathbf{x}, t) < 0$, $F(\mathbf{x}, t) = 0$ and $F(\mathbf{x}, t) > 0$ representing the interior, boundary and exterior of object, respectively. From the previous theorem, we know that if \mathbf{x}_0 is a grazing point on the smooth portion of boundary of $M(t)$, it satisfies

$$F(\mathbf{x}_0, t) = 0$$

$$F_t(\mathbf{x}_0, t) = 0$$

By Taylor's theorem, we can expand $F(\mathbf{x}_0, t_0)$ as follows:

$$F(\mathbf{x}_0, t_0) = F(\mathbf{x}_0, t_0 - \Delta t) + F_t(\mathbf{x}_0, t_0 - \Delta t)\Delta t + o(\Delta t) = 0$$

where Δt is positive and arbitrarily small. Hence

$$F(\mathbf{x}_0, t_0 - \Delta t) = -F_t(\mathbf{x}_0, t_0 - \Delta t)\Delta t + o(\Delta t)$$

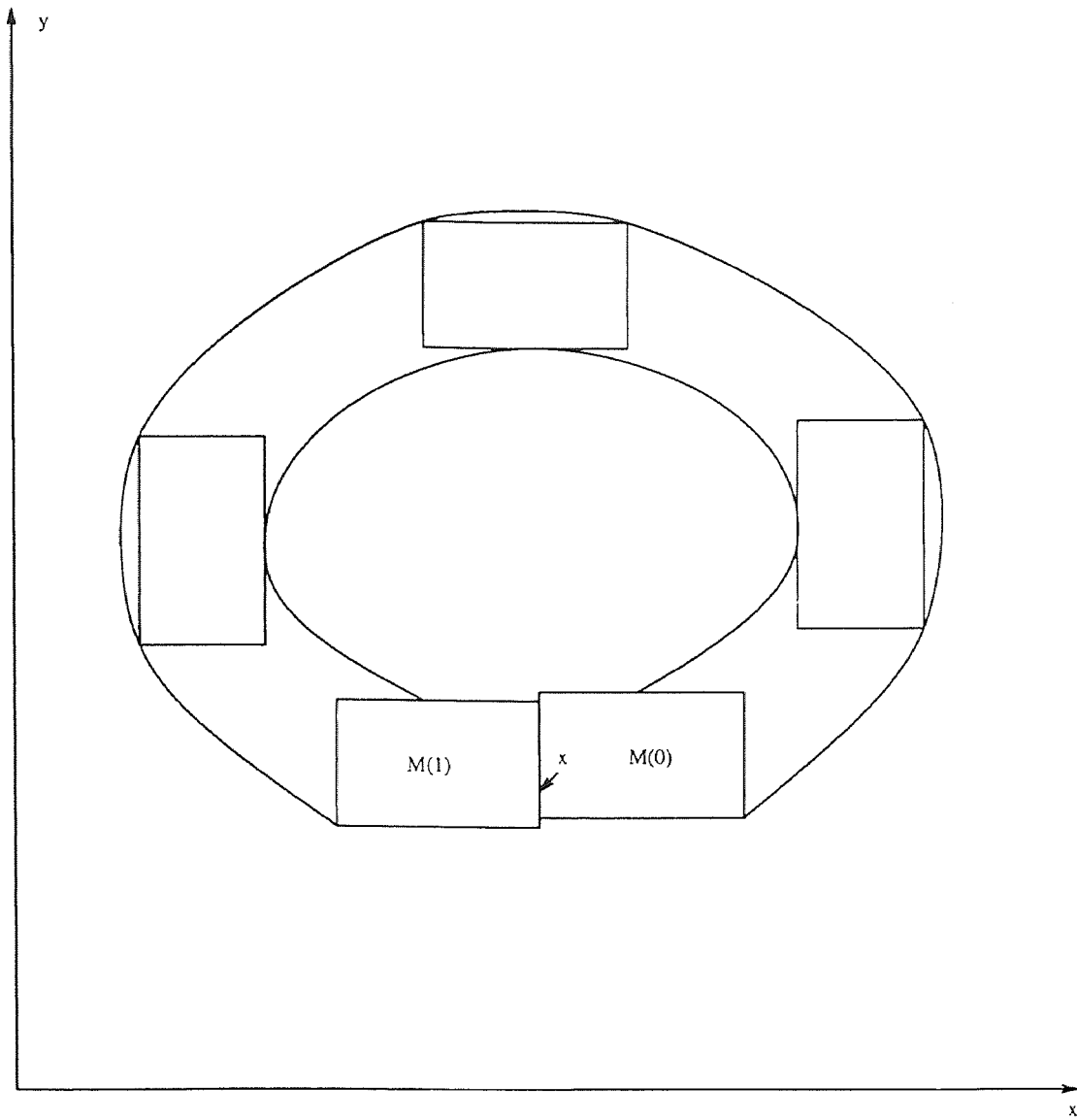


Figure 6 A 2-D example of singular case in the global trimming

So if $T(\mathbf{x}_0, t_0 - \Delta t) > 0$, from (11) and the fact that ∇F points out of M , we know that $F_t(\mathbf{x}_0, t_0 - \Delta t) > 0$, which implies that

$$F(\mathbf{x}_0, t_0 - \Delta t) < 0$$

This means that \mathbf{x}_0 belongs to the interior of the $M(t_0 - \Delta t)$, hence \mathbf{x}_0 is an interior point of the swept volume. This completes the proof.

We observe that when \mathbf{x}_0 is a grazing point of the smooth portion of $\partial M(t_0)$ one can also expand the Taylor series in another way:

$$\begin{aligned} F(\mathbf{x}_0, t_0 - \Delta t) &= F(\mathbf{x}_0, t_0) + F_t(\mathbf{x}_0, t_0)(-\Delta t) + \sum_{k=2}^N \frac{\partial^k}{\partial t^k} F(\mathbf{x}_0, t_0)(-\Delta t)^k + o(|\Delta t|^N) \\ &= \sum_{k=2}^N \frac{\partial^k}{\partial t^k} F(\mathbf{x}_0, t_0)(-\Delta t)^k + o(|\Delta t|^N) \end{aligned}$$

From which we can easily obtain the following result which is the “higher order criterion” Sambandan proved in [20].

Let a codimension-1 face f of the solid G in \mathbf{R}^n be given by an implicit equation $F(\mathbf{x}) = 0$ and let $F(\mathbf{x}) > 0$ denote the region in \mathbf{R}^n which is outside the solid generator. Let \mathbf{P} be a point on the face which satisfies the envelope criterion, i. e., $F(\mathbf{P}) = F_t(\mathbf{P}) = 0$. Then, there exists a neighborhood $U(\mathbf{P})$ of \mathbf{P} on the envelope of the face f , that will be on the boundary of or outside the swept volume if

$$\text{either } \frac{\partial^k F}{\partial t^k} = 0 \quad \forall k$$

or \exists an even integer $N > 0$ such that

$$\begin{aligned} 1. \quad \frac{\partial^k F}{\partial t^k} &= 0, k < N \\ 2. \quad \frac{\partial^N F}{\partial t^N} &> 0 \end{aligned}$$

i. e. , the first non-vanishing derivative must be of even order and be positive.

Hence \mathbf{P} is included in the type-2 patch (envelope curve). If N is even but the condition 2 is not satisfied, then $U(\mathbf{P})$ lies on the side of f that contains the swept volume and hence need not be included in the type-2 patch. If N is odd, $U(\mathbf{P})$ may lie partially in the swept volume.

It is instructive to compare Sambandan's local trimming procedure with that of Theorem 4.2. First, we observe that Theorem 4.2 applies to any grazing point on a smooth portion of $\partial M(t)$, whereas Sambandan's procedure is inconclusive if the first nonvanishing derivative is of odd order. Second, although theoretically possible, it may be very difficult to find $F(\mathbf{x}, t)$ for even a simple object M and sweep σ in practice. It is, in general, much easier to check the sign of $T(\mathbf{x}, t)$ than it is to compute $F(\mathbf{x}, t)$ and its various derivatives with respect to t .

CHAPTER 4
IMPLEMENTATION OF PROTOTYPE SOFTWARE IN 2-D
SPACE

In this chapter, we will describe the implementation of the theory developed in chapter 3 for evaluating the boundary representation of the swept volume generated by a planar polygonal object undergoing a general 2-D smooth rigid motion.

The given object M , which is a n -sided polygon, will be represented by a sequence of its vertices in the order in which they are encountered when marching counter-clockwise along its boundary. We observe that the configuration of the object at any time t , which is denoted as $M(t)$, is completely defined by the positions of its vertices, say $\{(x_i(t), y_i(t)), t \in [0, 1], i = 1, \dots, m\}$. The i th vertex of the polygon will be denoted by $\mathbf{v}_i(t)$ which is $(x_i(t), y_i(t))$, and the i th edge which represents the ordered pair $(\mathbf{v}_i(t), \mathbf{v}_{i+1}(t))$ is denoted by $\mathbf{e}_i(t)$

The general 2-D smooth sweep σ will be defined by the sweep equation or the sweep differential equation as follows:

$$\mathbf{x} = \xi(t) + A(t)\mathbf{x}_0 \quad (1)$$

$$\dot{\mathbf{x}} = X_\sigma = \dot{\xi} + \dot{A}(t)A^T(t)(\mathbf{x} - \xi) \quad (2)$$

where $\xi : [0, 1] \rightarrow \mathbf{R}^2$ and $A : [0, 1] \rightarrow \mathbf{SO}(2)$ are smooth and satisfy $\xi(0) = 0$, and $A(0) = I$. Here $\mathbf{x}_0 \in \mathbf{R}^2$ denotes the initial position of the point and $\mathbf{x} : [0, 1] \rightarrow \mathbf{R}^2$ the position of the point at time t . As we described in chapter 2, it is not difficult to derive (13) from (12). Here, we note that

$$\dot{\mathbf{x}} = \dot{\xi} + \dot{\theta} \begin{bmatrix} 0 & -1 \\ 1 & 0 \end{bmatrix} (\mathbf{x} - \xi) \quad (3)$$

since $A(t) = \begin{bmatrix} \cos \theta(t) & -\sin \theta(t) \\ \sin \theta(t) & \cos \theta(t) \end{bmatrix}$.

For the direction of the edge normals, we choose those which point into the interior of the polygon.

4.1 Overview of the Whole Process

The whole evaluation process can be outlined in detail as follows:

- Step 1** Given: the polygonal object M , a smooth 2-D sweep which is represented by sweep differential equation

$$\dot{\mathbf{x}} = X_\sigma = \dot{\xi}(t) + \dot{A}A^T(\mathbf{x} - \xi)$$

and the time interval $[0, 1]$.

- Step 2** For each edge e_i , compute the edge normals (normalized, inward directed) at time 0, which are denoted by $N_i(\mathbf{x}, 0)$. We note that all of these normals are constant on e_i (which is a straight line segment).

- Step 3** Subdivide the time interval $[0, 1]$ into a finite number of segments which are represented by a sequence of time instants.

- Step 4** At time $t = 0$, compute the instantaneous ingress portion of $\partial M(0)$ which may be composed of several ingress boundary curves. Discretize them into a finite number of straight line segments and determined by a set of ingress points.

- Step 5** For each time instant, compute the instantaneous grazing points of $\partial M(t)$ and note their geometric relationship. By making use of the geometric relationship

between these grazing points, form a set of grazing boundary curves.

Step 6 At time $t = 1$, compute the instantaneous egress portion of $\partial M(1)$ which may be composed of several egress boundary curves. Discretize them into a finite number of straight line segments which are determined by a set of egress points.

Step 7 Collect the points and curves obtained in steps 4, 5 and 6. These are the candidate boundary points and candidate boundary curves.

Step 8 Global trimming:

(1) **Initial global trimming:** eliminate those candidate boundary points which belong to the interior of the swept volume $S_\sigma(M) = \bigcup_{t=0}^1 M(t)$.

(2) **Secondary global trimming:** If a candidate point belongs to the boundary of more than one t -section of the swept volume and has not been eliminated by initial trimming, it may still need to be removed. If its normal vectors for two of the sections are in opposite directions, it should be trimmed. This occurs when the inner product of the two normal vectors equals -1 .

Step 9 Connect the remaining candidate boundary curves to form an approximation of the boundary representation of the swept volume.

We will discuss some steps in detail in the next section and the following example will be used to illustrate the steps.

Example 4.1 The object is the pentagon shown in figure 8. and the swept volume produced is shown in figure 9.

Object description:

$$(0,0) \rightarrow (2.0,0) \rightarrow (2.0,0.5) \rightarrow (1.0,1.5) \rightarrow (0.0,1.0)$$

This is the sequence of vertex points in the counter-clockwise orientation.

Sweep equation:

$$\begin{bmatrix} x \\ y \end{bmatrix} = \begin{bmatrix} 4t \\ 0 \end{bmatrix} + \begin{bmatrix} \cos(\pi t) & -\sin(\pi t) \\ \sin(\pi t) & \cos(\pi t) \end{bmatrix} \begin{bmatrix} x_0 \\ y_0 \end{bmatrix}$$

Sweep differential equation:

$$\begin{bmatrix} \dot{x} \\ \dot{y} \end{bmatrix} = \begin{bmatrix} 4 \\ 0 \end{bmatrix} + \begin{bmatrix} -\pi y \\ \pi(x - 4t) \end{bmatrix}$$

4.2 Implementation of Candidate Points Selection Procedure

Here, we will describe in detail how to apply the sweep flow method to obtain a set of candidate boundary points, and join them into candidate boundary curves by making use of their geometric relationship. Let $T(\mathbf{x}, t)$ denote the dot product of the sweep vector and the normal vector at \mathbf{x} on the boundary of $M(t)$ at time t , which is defined by equation (1).

As we can see from equation (1), in order to determine the value of $T(\mathbf{x}, t)$, the edge normal $N(\mathbf{x}, 0)$ needs to be computed. This is quite easily done as follows: Let $\mathbf{x} \in \mathbf{e}_i$ and define

$$N^*(\mathbf{x}) = (v_{i+1}(0) - v_i(0)) \begin{bmatrix} 0 & 1 \\ -1 & 0 \end{bmatrix}$$

Then

$$N(\mathbf{x}, 0) = N^*(\mathbf{x}) / \|N^*(\mathbf{x})\|$$

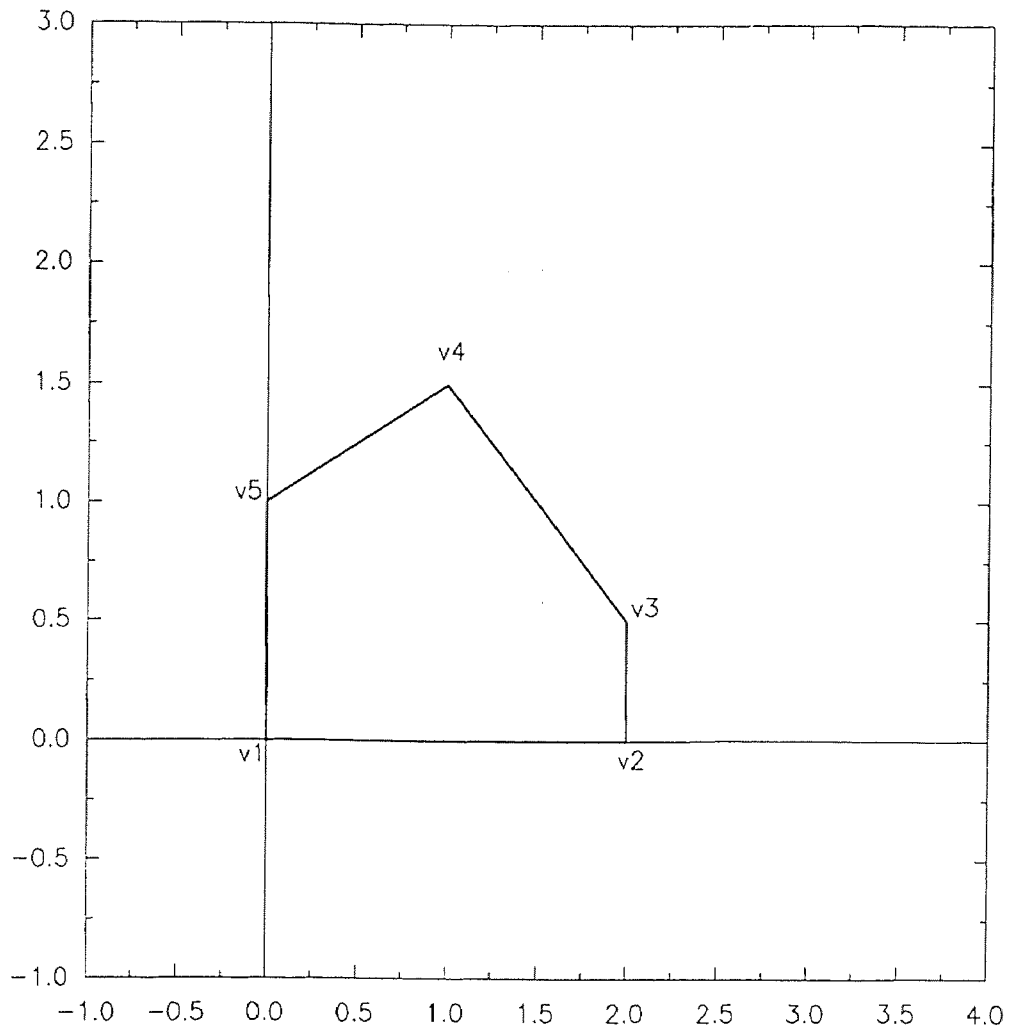


Figure 8 The object in example 4.1

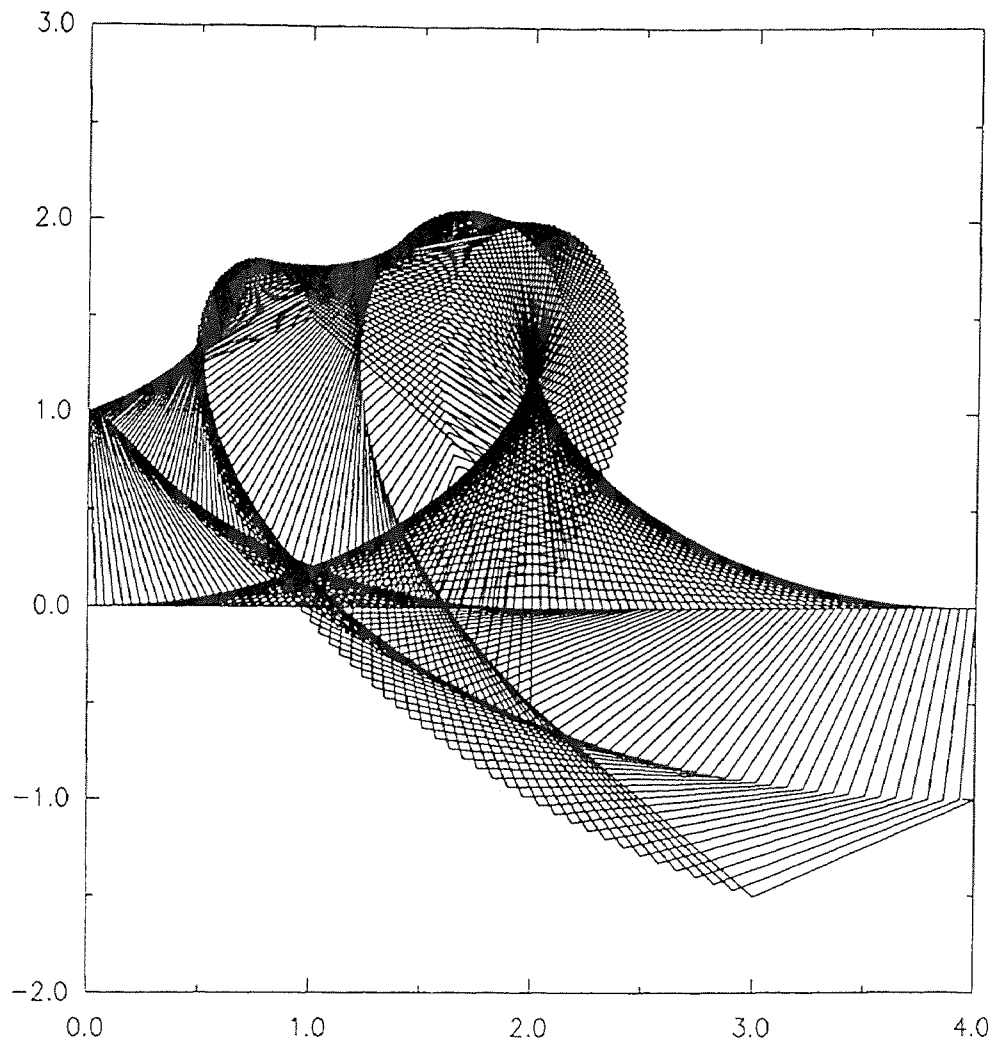


Figure 9 The swept volume in example 4.1

The following result characterizes the grazing point sets on the edges of the object being swept.

Lemma 4.1 *Given a smooth 2-D sweep and a polygonal object. At any given time $t \in [0, 1]$, one and only one of the following is true for an edge excluding the vertices: there is exactly one grazing point; or there are no grazing points; or every point is a grazing point.*

Proof. As we mentioned before, at any given time t , for each edge e_i except at its two vertices, the normal vector is constant which can be expressed as: $N_i(t) = (N_1(t), N_2(t))$. From equation (14), the sweep vector at any given point \mathbf{x} and time t is:

$$\begin{aligned} X_\sigma &= \dot{\xi}(t) + \dot{\theta}(t) \begin{bmatrix} 0 & -1 \\ 1 & 0 \end{bmatrix} (\mathbf{x}(t) - \xi(t)) \\ &= \begin{bmatrix} \dot{\xi}_1 \\ \dot{\xi}_2 \end{bmatrix} + \dot{\theta} \begin{bmatrix} 0 & -1 \\ 1 & 0 \end{bmatrix} \begin{bmatrix} (x_1 - \xi_1) \\ (x_2 - \xi_2) \end{bmatrix} \\ &= \begin{bmatrix} \dot{\xi}_1 + \dot{\theta}(\xi_2 - x_2) \\ \dot{\xi}_2 + \dot{\theta}(x_1 - \xi_1) \end{bmatrix} \end{aligned}$$

If \mathbf{x} is a grazing point on the interior of an edge e_i at given time t , it must satisfy the tangency condition:

$$\begin{aligned} T(\mathbf{x}, t) &= \langle X_\sigma, N_i \rangle \\ &= \dot{\theta} N_2 x_1 - \dot{\theta} N_1 x_2 + N_1(\xi_1 + \dot{\theta} \xi_2) + N_2(\xi_2 - \dot{\theta} \xi_1) = 0 \end{aligned} \quad (4)$$

Since \mathbf{x} is on the edge e_i , it must satisfy the edge equation which is in the form:

$$ax_1 + bx_2 = c \quad (5)$$

In which a , b and c are constants for t fixed.

Equations (16) and (17) constitute a pair of linear equations in the two unknowns x_1, x_2 at time t . The determinant of this system is:

$$Det = \det \begin{bmatrix} N_2 \dot{\theta} & -N_1 \dot{\theta} \\ a & b \end{bmatrix}$$

$$\begin{aligned}
&= \dot{\theta}(N_2b + N_1a) \\
&= \dot{\theta}K
\end{aligned}$$

Where $K = N_2b + N_1a \neq 0$. If $\dot{\theta} \neq 0$, this linear system has unique solution $\mathbf{x} = (x_1, x_2)$, which means that in this case the grazing point on edge \mathbf{e}_i is unique if exists (it does not exist if the point lies on the line (17) outside the edge). If $\dot{\theta} = 0$, (16) and (17) either have no solution, or every point of the line (17) is a solution. Thus the proof is complete.

It follows from Theorem 3.2 proved in chapter 3 that the following procedure will yield all of the candidate boundary points.

At time 0, compute the normal vector $N_i(\mathbf{x}, 0)$ of each edge \mathbf{e}_i . Let $T_i(\mathbf{v}_j, t)$ denote the dot product of the sweep vector at vertex \mathbf{v}_j and the normal vector of edge \mathbf{e}_i at time t . At any time t , for each edge $\mathbf{e}_i = (\mathbf{v}_i(t), \mathbf{v}_{i+1}(t))$, compute $T_i(\mathbf{v}_i, t)$ and $T_i(\mathbf{v}_{i+1}, t)$.

For each edge \mathbf{e}_i , check the signs of $T_i(\mathbf{v}_i, t)$ and $T_i(\mathbf{v}_{i+1}, t)$:

- If they are both greater than or equal to zero, then this edge as a whole belongs to the ingress portion of $\partial M(t)$
- If they are both less than or equal to zero, then this edge belongs to the egress portion of $\partial M(t)$
- If $T_i(\mathbf{v}_i, t) \cdot T_i(\mathbf{v}_{i+1}, t) < 0$, then we can use some standard numerical algorithm (e. g. bisection method) to find the grazing point \mathbf{x} on the edge \mathbf{e}_i which satisfies $T(\mathbf{x}, t) = 0$. The portion from \mathbf{x} to the vertex satisfying $T < 0$ is the egress portion of this edge, and the other side is the ingress part.

At any time t , each vertex can be classified as follows:

- If $T_i(\mathbf{v}_i, t) > 0$ and $T_{i+1}(\mathbf{v}_i, t) > 0$, this vertex is an ingress point.
- If $T_i(\mathbf{v}_i, t) < 0$ and $T_{i+1}(\mathbf{v}_i, t) < 0$, this vertex is an egress point.

- If $T_i(\mathbf{v}_i, t) \cdot T_{i+1}(\mathbf{v}_i, t) \leq 0$, it is a grazing point.

This classification is directly based on the definition we stated in chapter 2. The candidate boundary points of example 4.1 are shown in figure 10.

In order to improve the efficiency, it is also very important to exploit the geometric relationship between the candidate points in order to save the computational work of forming the final boundary representation of the swept volume. The following properties of the candidate boundary points are very useful:

- During the sweep, the grazing point of an edge will move along the edge. Usually it will start at one of the end points and move to the other end. However, the grazing point may start at an end and terminate at an intermediate point or begin at an intermediate point and end at a vertex, or even start and end at intermediate points. In any case, if we connect the grazing points of this edge according to their movement along the edge as it moves through successive instants of time, we obtain an edge candidate curve.
- Because of the multiple normals at a vertex, there exist some time intervals $[t_i, t_j]$ in which the vertex is a candidate point. The trajectories of this vertex during those time intervals are the vertex candidate curves.

In the actual implementation, we use a double link structure to keep a record of the geometric information connecting the candidate points. The link will be changed during the global trimming procedure described below.

4.3 Implementation of Trimming Procedure

In the 2-D case, global trimming requires a procedure for determining whether or not a given candidate point lies within the interior of any of the polygonal t -sections $M(t)$, $0 \leq t \leq 1$. This can be done by using following algorithm:

Algorithm 4.1 *Given any polygon and a point in 2-D space, draw a ray from this point in any direction (for convenience and efficiency, we adopt the upward direction*

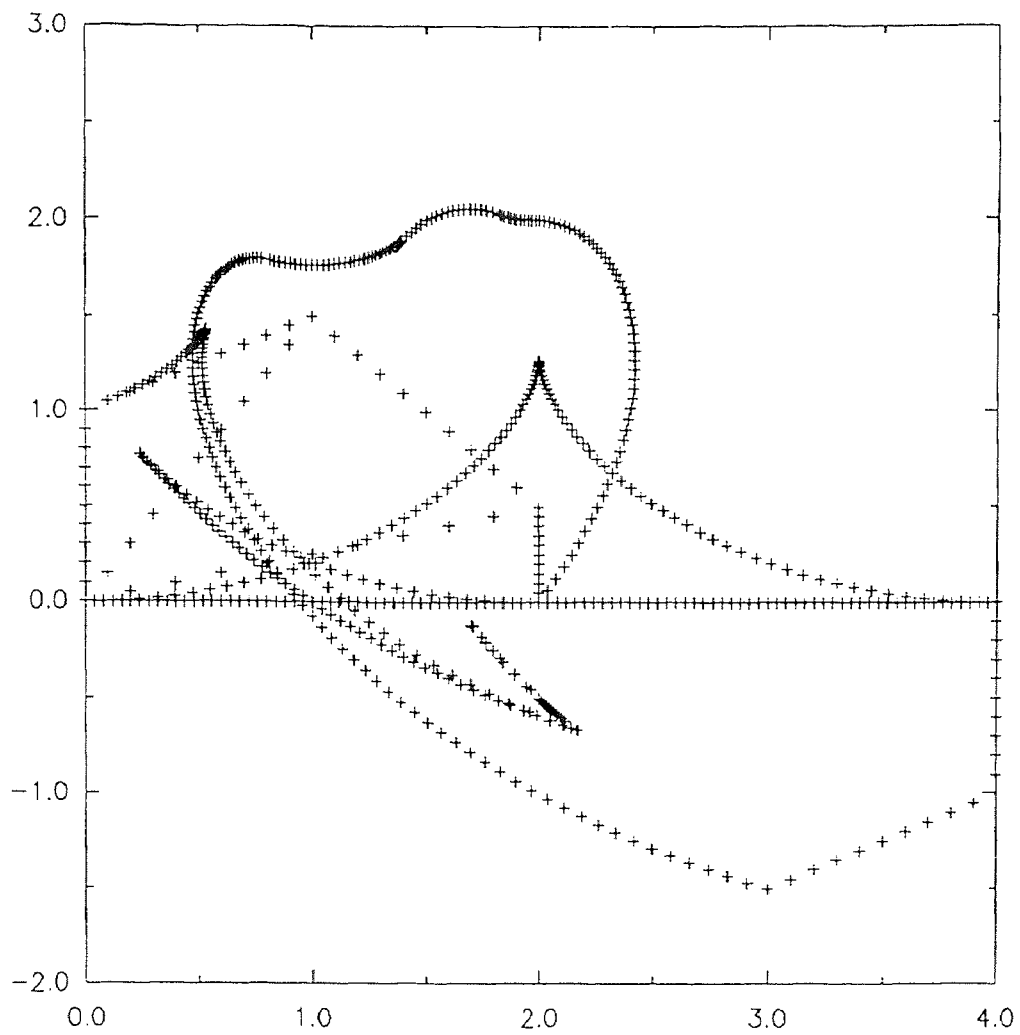
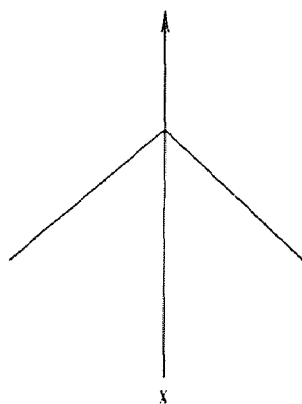
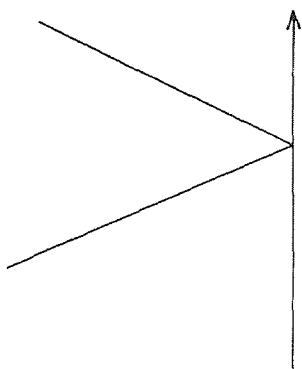


Figure 10 The candidate boundary points of example 4.1

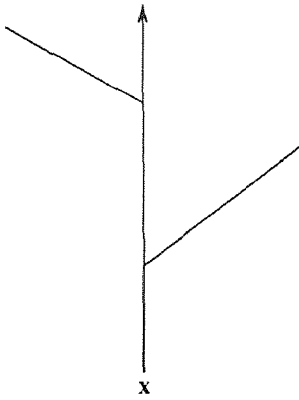
or downward direction). Count the number of intersections of the ray with the edges of polygon. If this number is odd, then the point is inside the polygon; if it is even, then it is outside the polygon. See figure 11. The count of the number of intersections is done as follows: If the intersection does not coincide with the vertex of the edge, add 1 to the intersection counter; Otherwise, there are the special cases for which the count must be defined according to the following illustrations:



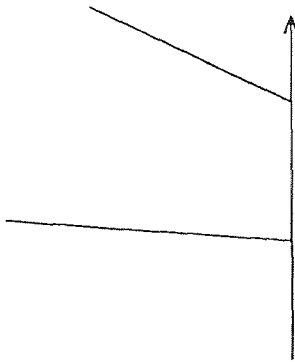
case 1.1 Intersection with a vertex. If the two edges are on different sides of the ray starting at x , add 1 to the intersection counter.



case 1.2 Intersection with a vertex. If the two edges are on the same side of the ray starting at x , add 2 to the x intersection counter.



case 2.1 Complete intersection with an edge. If two adjacent edges are on different sides of the ray starting at \mathbf{x} , add 1 to the intersection counter.



case 2.2 Complete intersection with edge. If two adjacent edges are on the same side of \mathbf{x} , add 2 to the \mathbf{x} intersection counter.

Although a proof of this theorem can be obtained using quite basic results from topology, we have not been able to find a complete proof in the literature. In the interest of completeness, a proof is given in Appendix A at the end of this thesis.

Thus the global trimming procedure can be outlined as follow:

Input: The set of candidate boundary points

Global trimming:

Initial global trimming: For each candidate boundary point, use the algorithm 4.1 to test whether it belongs to the interior of $M(t)$ for some $t \in [0, 1]$. If it

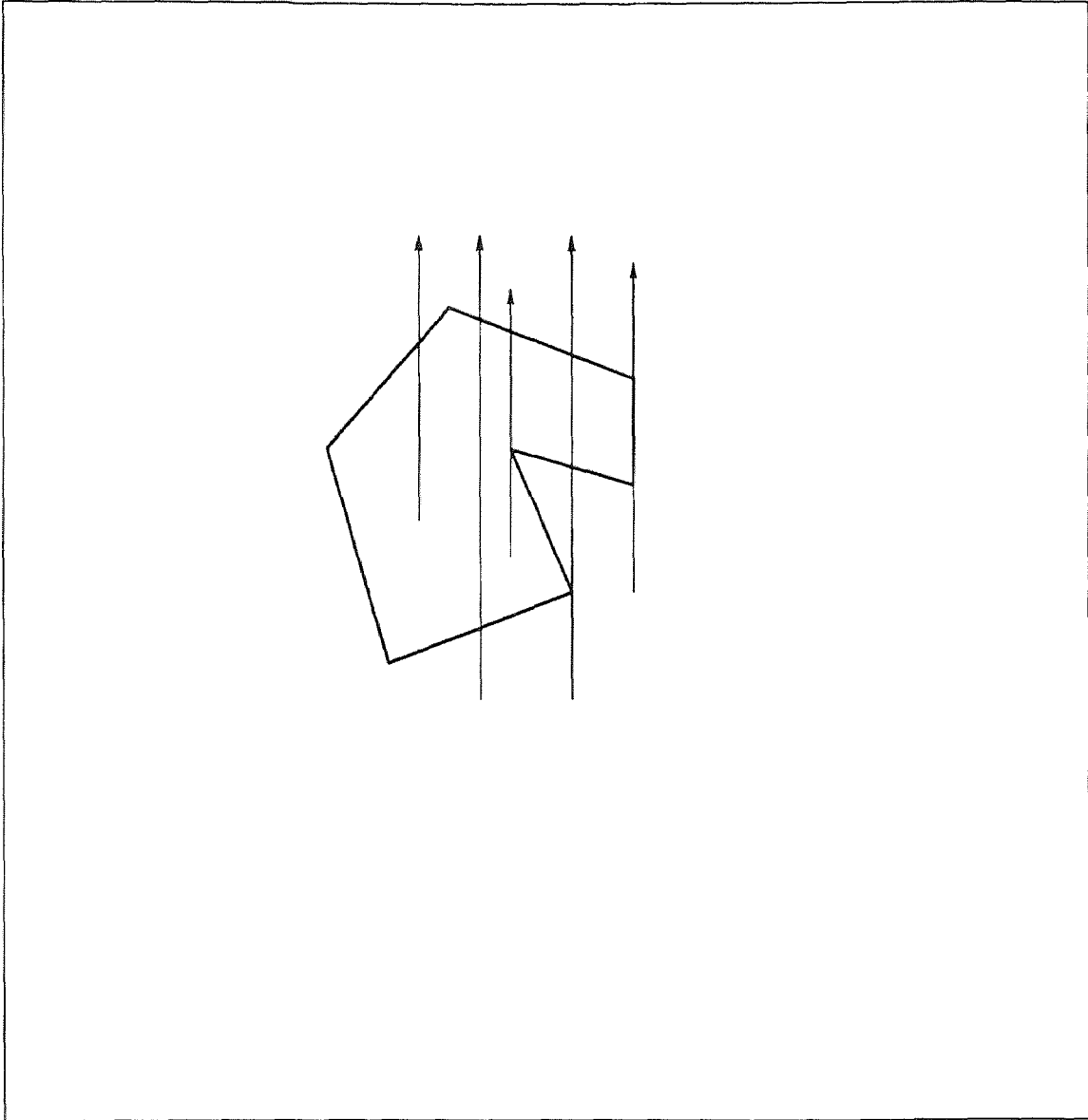


Figure 11 Deciding whether a point is inside a polygon or not

does, eliminate it from the candidate boundary point set. Otherwise, record the number of times it belong to $\partial M(t)$ for some $t \in [0, 1]$.

Secondary global trimming: For each candidate boundary point left after initial global trimming, check if it belongs to the boundary of more than one t -section of the swept volume. If it does, then compute dot products of the its normals at all the different time instances, If one of them is equal to -1 , this point is a singular candidate point and should be trimmed.

Output: The set of boundary points

From the set of boundary points constructed by our algorithm, one can obtain a piecewise linear approximation to the boundary of the swept volume by linear interpolation (i. e. just connect successive points by straight line segments). It is clear that the precision of this approximation can be controlled by the choice of the subdivision of $[0, 1]$ into time instants. Figure 12 the trimming result of example 4.1 and the final boundary representation is shown in figure 13.

4.4 Some Examples

Example 4.1 Figure 14–17 shows a pentagon undergoing a sweep for which the swept volume produced has a hole, which means that the boundary of the swept volume has more than one connected component.

Object description:

$$(0, 0) \rightarrow (2.0, 0) \rightarrow (2.0, 0.5) \rightarrow (1.0, 1.5) \rightarrow (0.0, 1.0)$$

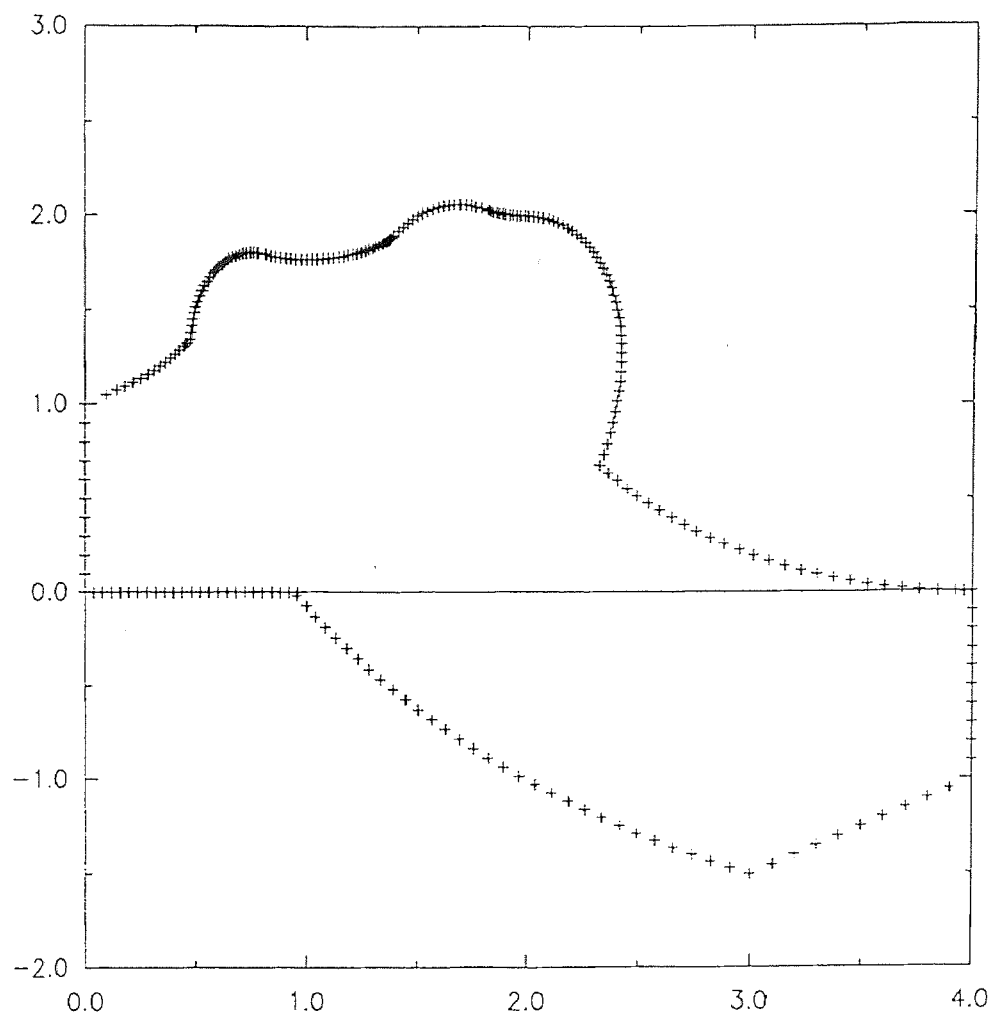


Figure 12 The boundary points after global trimming of example 4.1

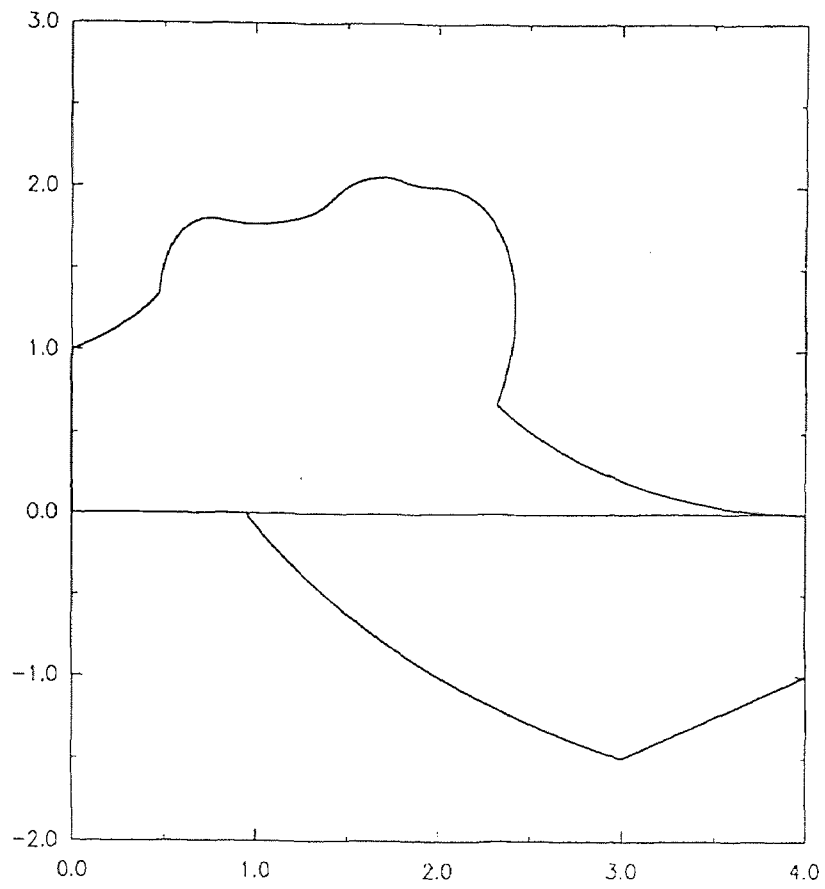


Figure 13 The final boundary of the swept volume of example 4.1

Sweep equation:

$$\begin{bmatrix} x \\ y \end{bmatrix} = \begin{bmatrix} 4t \\ 4(t-0.5)^2 - 1 \end{bmatrix} + \begin{bmatrix} \cos(3\pi t) & -\sin(3\pi t) \\ \sin(3\pi t) & \cos(3\pi t) \end{bmatrix} \begin{bmatrix} x_0 \\ y_0 \end{bmatrix}$$

Sweep differential equation:

$$\begin{bmatrix} \dot{x} \\ \dot{y} \end{bmatrix} = \begin{bmatrix} 4 \\ 8(t-0.5) \end{bmatrix} + \begin{bmatrix} -3\pi(y - 4(t-0.5)^2 + 1) \\ 3\pi(x - 4t) \end{bmatrix}$$

Example 4.2 In this example, we approximate a disk by a polygon, and thus obtain an approximation of its swept volume.

Object description:

A disk of radius 1 whose boundary is a circle approximated by a polygon:

$(1.0, 0.0) \rightarrow (0.707, 0.707) \rightarrow (0.0, 1.0) \rightarrow (-0.707, 0.707) \rightarrow (-1.0, 0.0) \rightarrow$

$(-0.707, -0.707) \rightarrow (0.0, -1.0) \rightarrow (0.707, -0.707)$

Sweep equation:

$$\begin{bmatrix} x \\ y \end{bmatrix} = \begin{bmatrix} 4t \\ 0 \end{bmatrix} + \begin{bmatrix} \cos(\pi t) & -\sin(\pi t) \\ \sin(\pi t) & \cos(\pi t) \end{bmatrix} \begin{bmatrix} x_0 \\ y_0 \end{bmatrix}$$

Sweep differential equation:

$$\begin{bmatrix} \dot{x} \\ \dot{y} \end{bmatrix} = \begin{bmatrix} 4 \\ 0 \end{bmatrix} + \begin{bmatrix} -\pi y \\ \pi(x - 4t) \end{bmatrix}$$

The results are shown in figures 18–21.

Example 4.3 Figures 22–25 are the same example which appears on the page 58 of [20].

Object description:

$(-1.0, 0.0) \rightarrow (1.0, 0.0) \rightarrow (1.5, 1.0) \rightarrow (0.0, 2.0) \rightarrow (-1.5, 1.0)$

Sweep equation:

$$\begin{bmatrix} x \\ y \end{bmatrix} = \begin{bmatrix} 5t \\ 5t \end{bmatrix} + \begin{bmatrix} \cos(2.7\pi t) & -\sin(2.7\pi t) \\ \sin(2.7\pi t) & \cos(2.7\pi t) \end{bmatrix} \begin{bmatrix} x \\ y \end{bmatrix}$$

Sweep differential equation:

$$\begin{bmatrix} \dot{x} \\ \dot{y} \end{bmatrix} = \begin{bmatrix} 5.0 \\ 5.0 \end{bmatrix} + \begin{bmatrix} -2.7(y - 5.0t) \\ 2.7(x - 5.0t) \end{bmatrix}$$

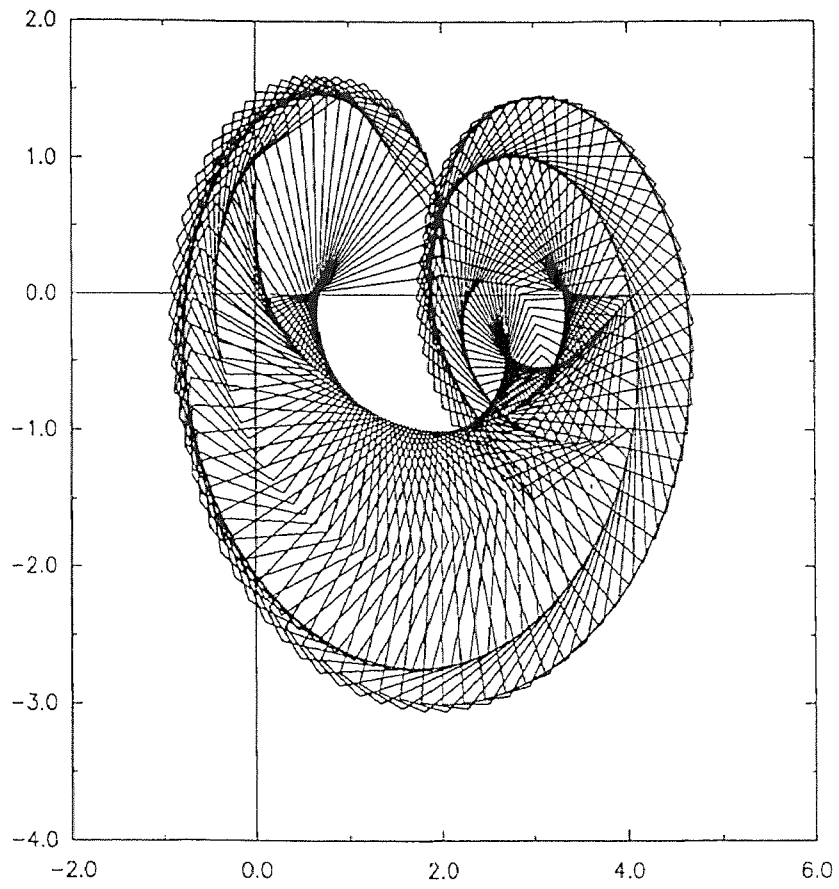


Figure 14 The swept volume of example 4.2

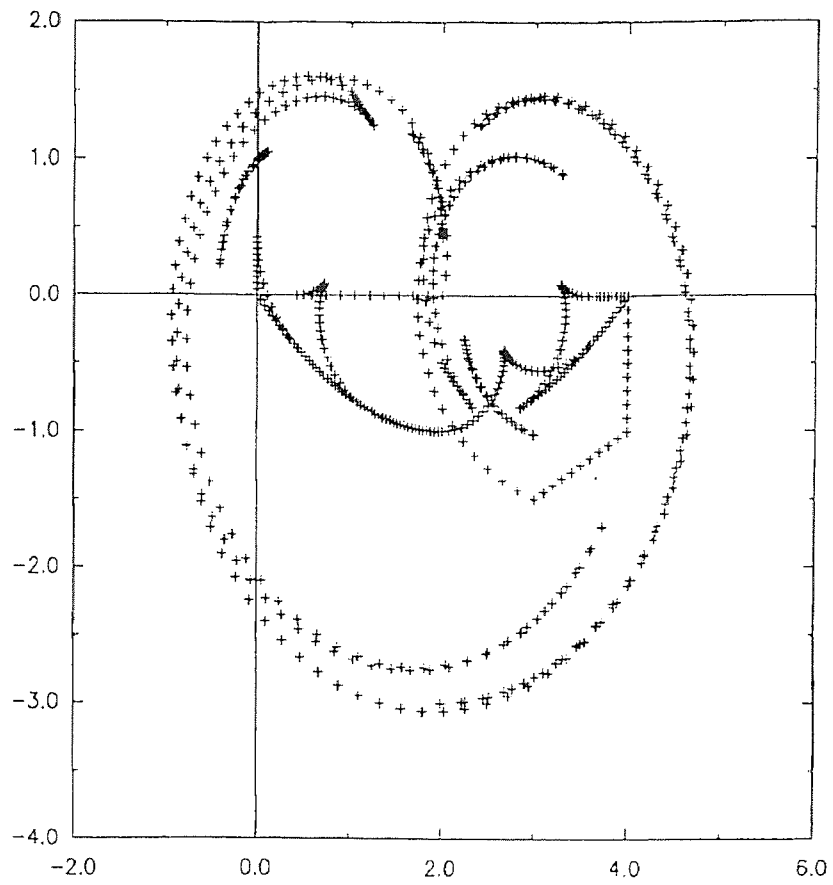


Figure 15 The candidate boundary points of example 4.2

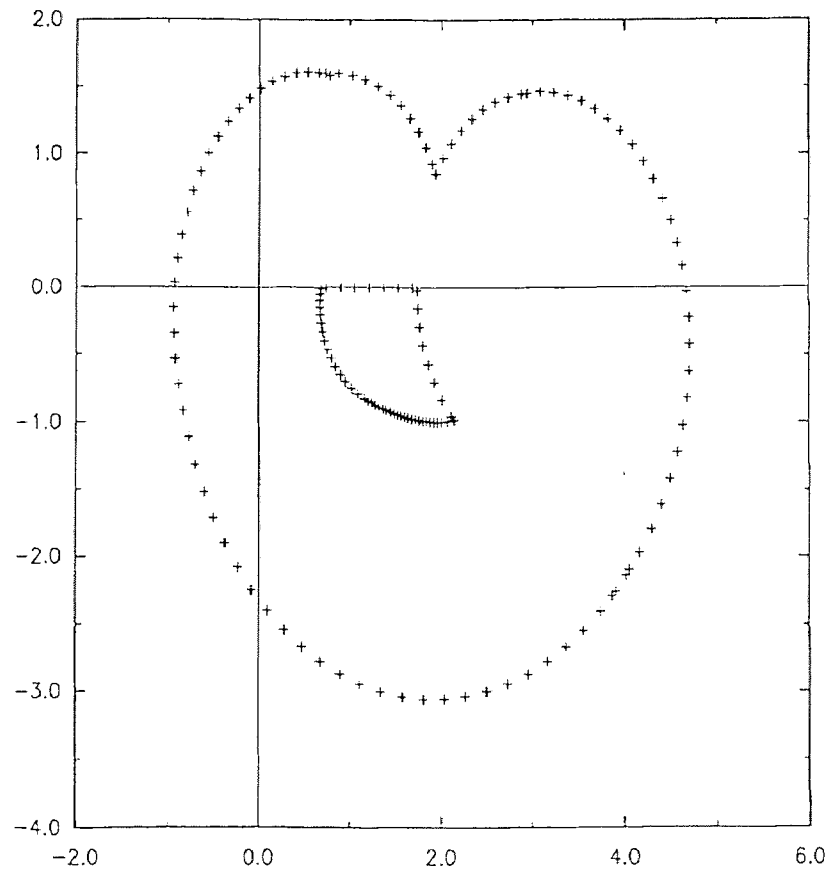


Figure 16 The boundary points after global trimming of example 4.2

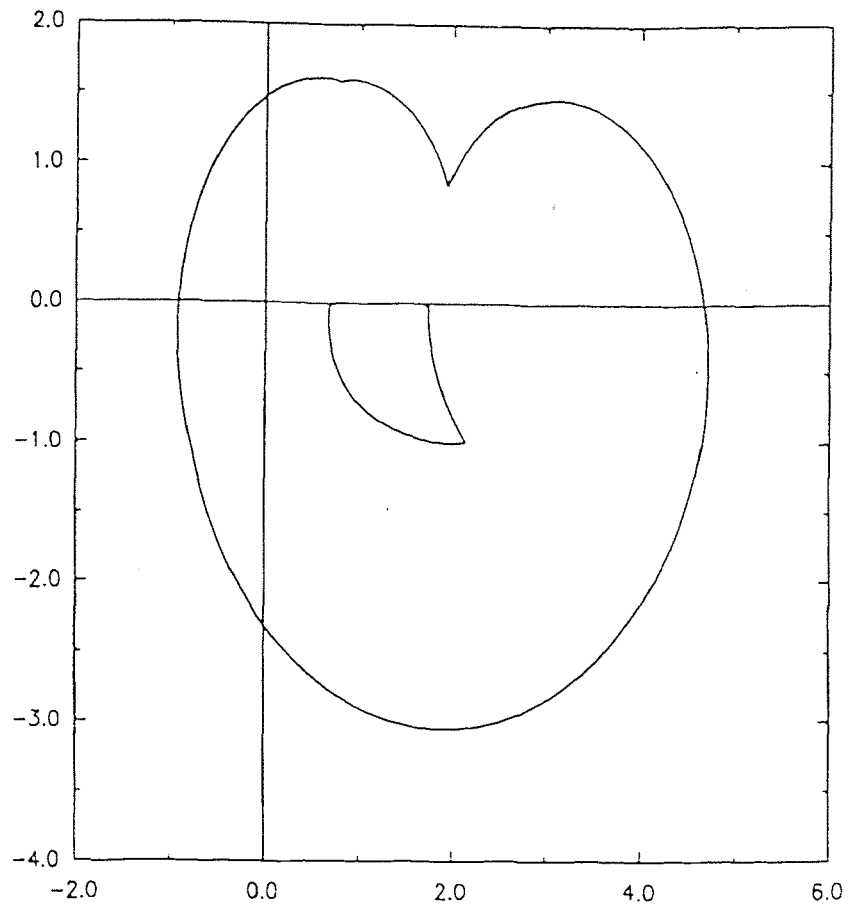


Figure 17 The boundary representation of swept volume in example 4.2

Missing Page

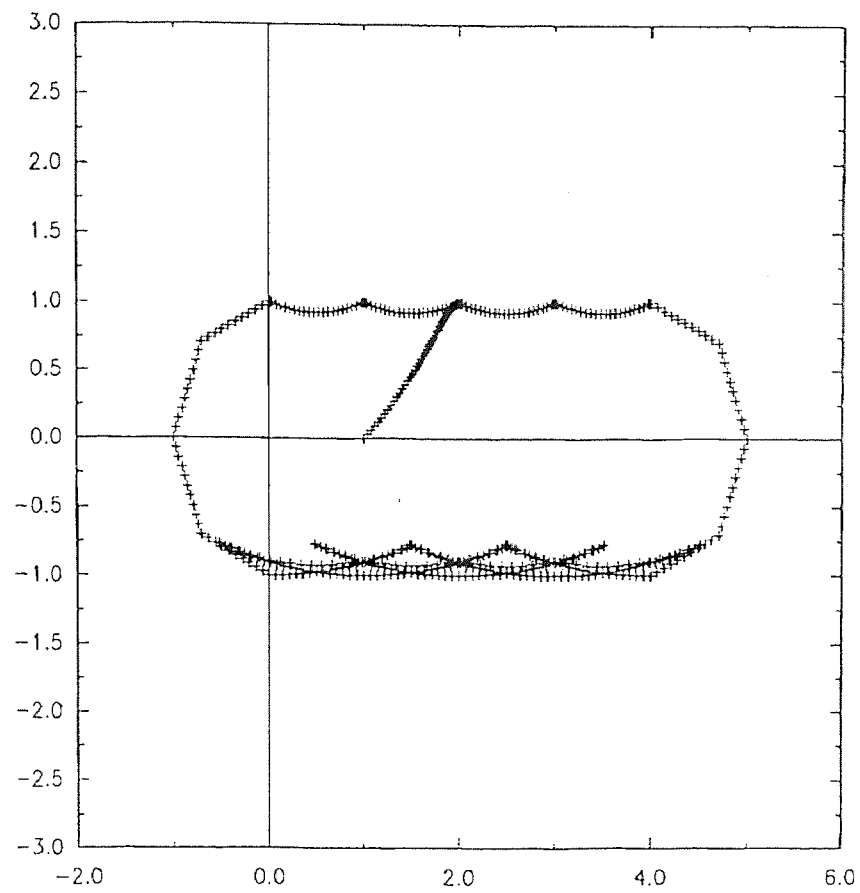


Figure 19 The candidate boundary points of example 4.3

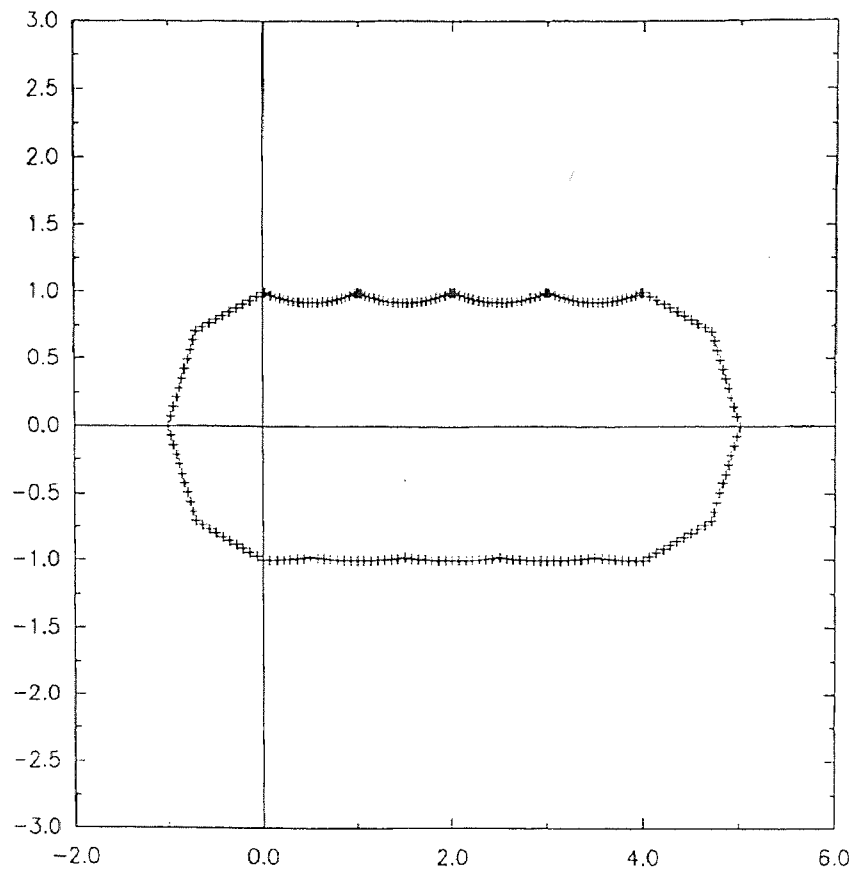


Figure 20 The boundary points after global trimming of example 4.3

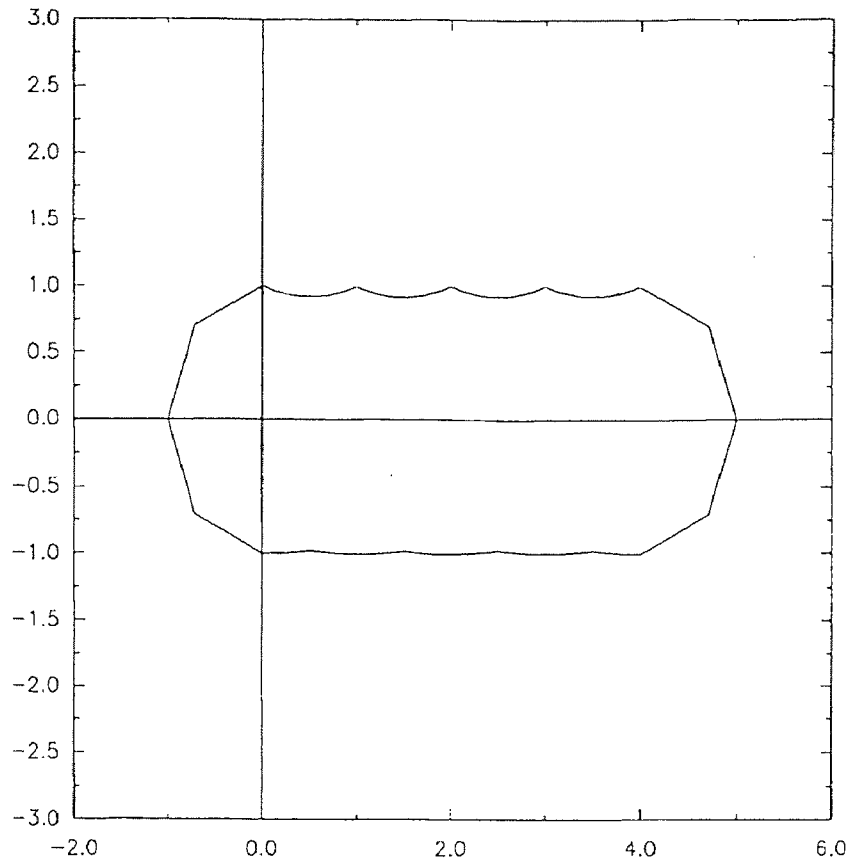


Figure 21 The boundary representation of swept volume in example 4.3

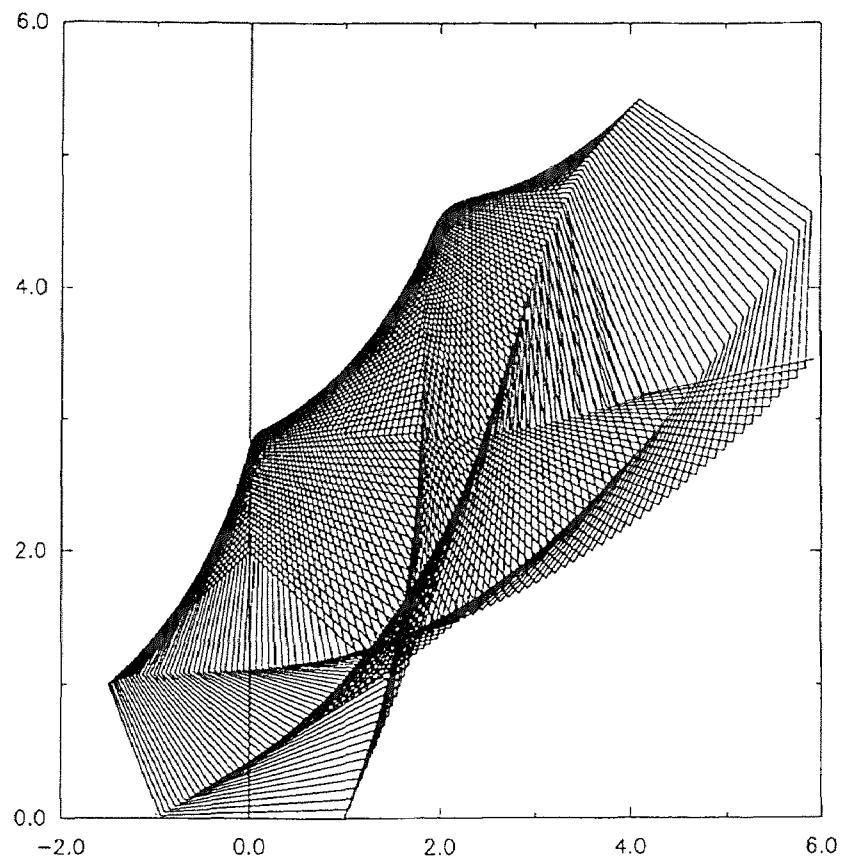


Figure 22 The swept volume of example 4.4

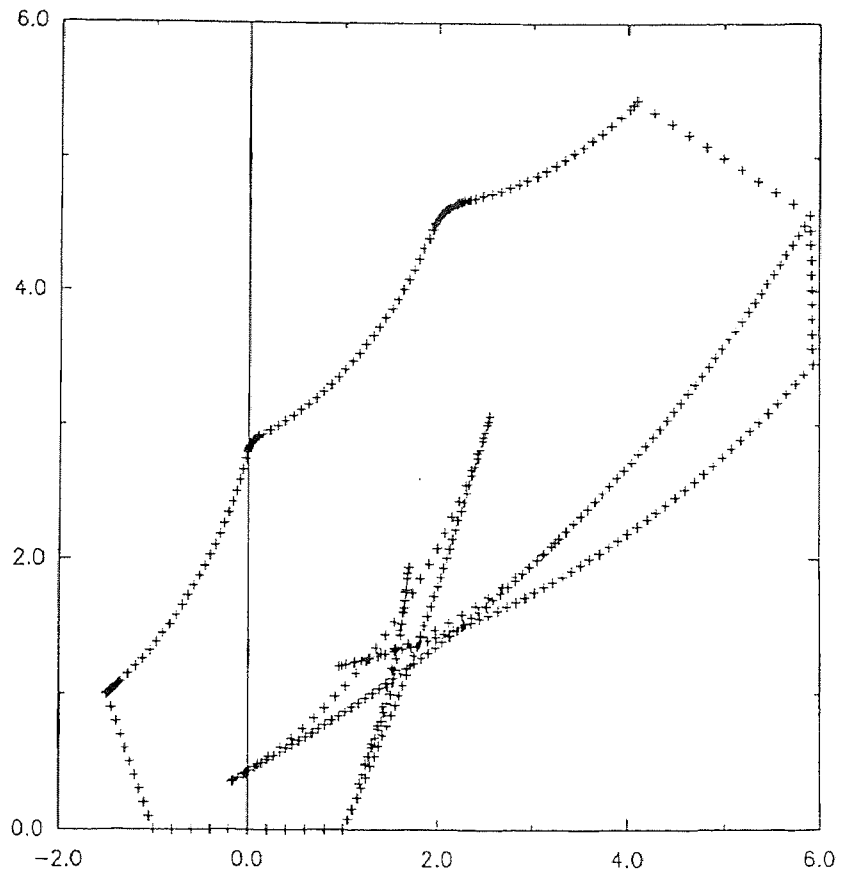


Figure 23 The candidate boundary points of example 4.4

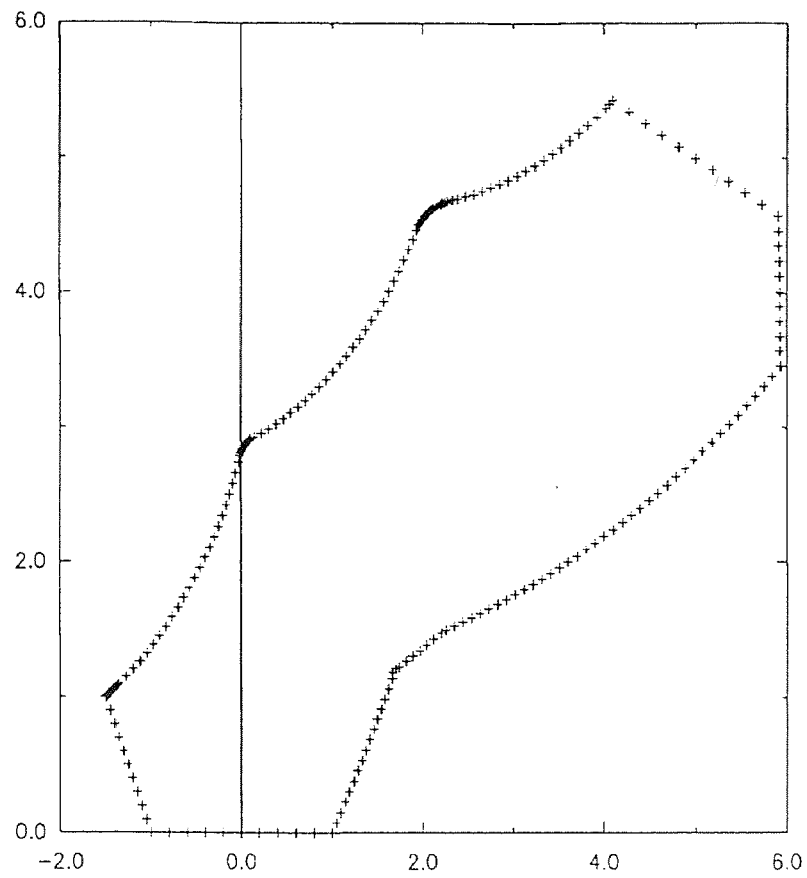


Figure 24 The boundary points after global trimming of example 4.4

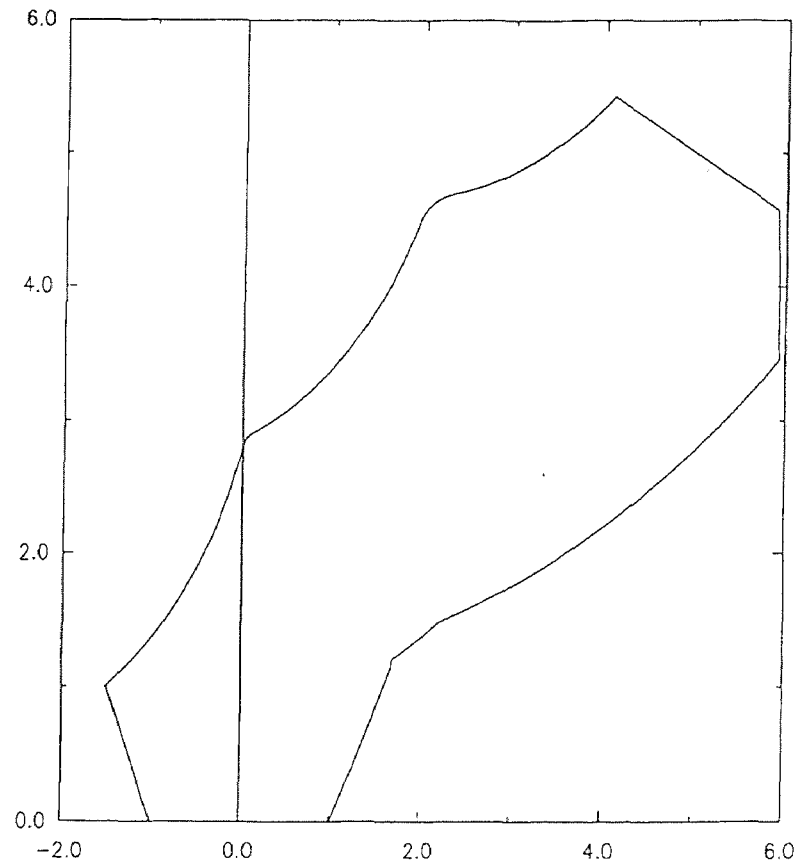


Figure 25 The boundary representation of swept volume in example 4.4

CHAPTER 5

SOME IDEAS ON 3-D EXTENSIONS

In this chapter, we will briefly describe how our general solution procedure can be applied to 3-D space. Although our sweep flow method has no restriction on the shape of the object, we still want to concentrate our attention on polyhedra because they are more readily handled. We note that any reasonably smooth 3-D object can be approximated by a polyhedron to any precision. The resulting boundary representation of the swept volume is then a close approximation to the actual swept volume boundary.

We will use the boundary-based, object-based, evaluated-form of representation of solid models to model the polyhedral object we want to sweep. There are several data structures which can be used to represent the topological information of the solid models. We plan to use the edge-based graph data structures which include the well known winged-edge structure [1] and its variations. For more details, refer to [27].

The general smooth 3-D sweep and sweep differential equation will also be represented as:

$$\mathbf{x} = \xi(t) + A(t)\mathbf{x}_0 \tag{1}$$

$$\dot{\mathbf{x}} = \dot{X}_\sigma = \dot{\xi} + \dot{A}(t)A^T(t)(\mathbf{x} - \xi) \tag{2}$$

Where $\xi : [0, 1] \rightarrow \mathbf{R}^3$ and $A : [0, 1] \rightarrow \mathbf{SO}(3)$ are smooth and satisfy $\xi(0) = 0$, and $A(0) = I$. Here $\mathbf{x}_0 \in \mathbf{R}^3$ denotes the initial position of the point and $\mathbf{x} : [0, 1] \rightarrow \mathbf{R}^3$ the position of the point at time t . As we described in chapter 2, it is not difficult to derive (19) from (18). For the six degrees of freedom of 3-D Euclidean motions, the

sweep equation is:

$$\begin{aligned} \mathbf{x} &= \boldsymbol{\xi}(t) + A(t)\mathbf{x}_0 \\ &= \begin{bmatrix} \xi_1(t) \\ \xi_2(t) \\ \xi_3(t) \end{bmatrix} + \begin{bmatrix} c\alpha c\beta & c\alpha s\beta s\gamma - s\alpha c\gamma & c\alpha s\beta c\gamma + s\alpha s\gamma \\ s\alpha c\beta & s\alpha s\beta s\gamma + c\alpha c\gamma & s\alpha s\beta c\gamma - c\alpha s\gamma \\ -s\beta & c\beta s\gamma & c\beta c\gamma \end{bmatrix} \mathbf{x}_0 \end{aligned}$$

Where $c\alpha = \cos \alpha$, $s\alpha = \sin \alpha$, etc., $\xi_1(t), \xi_2(t), \xi_3(t)$ are the three components of the translational motion with respect to the fixed world coordinate system, and α, β, γ are the euler angles which specify the rotation angles of the object with respect to its original orientation. With some computational work, the sweep differential equation can be shown to have the following form:

$$\begin{aligned} \dot{\mathbf{x}} &= X_\sigma = \dot{\boldsymbol{\xi}} + \dot{A}(t)A^T(t)(\mathbf{x} - \boldsymbol{\xi}) \\ &= \begin{bmatrix} \dot{\xi}_1(t) \\ \dot{\xi}_2(t) \\ \dot{\xi}_3(t) \end{bmatrix} + \begin{bmatrix} 0 & -\dot{\alpha} + \dot{\gamma}s\alpha & \dot{\beta}c\alpha + \dot{\gamma}s\alpha c\beta \\ \dot{\alpha} - \dot{\gamma}s\beta & 0 & \dot{\beta}s\alpha - \dot{\gamma}c\alpha c\beta \\ -\dot{\beta} - \dot{\gamma}s\alpha c\beta & -\dot{\beta}s\alpha + \dot{\gamma}c\alpha c\beta & 0 \end{bmatrix} \begin{bmatrix} \mathbf{x}_1 - \xi_1 \\ \mathbf{x}_2 - \xi_2 \\ \mathbf{x}_3 - \xi_3 \end{bmatrix} \end{aligned}$$

Our 3-D evaluation process, which is also based on the general process described in chapter 3, is similar to the 2-D case, but is much more complicated. We describe it briefly as follows:

- **Step 1.** Input the polyhedral object M , a smooth 3-D sweep which is represented by sweep equation or sweep differential equation in the form of (1) and (2), and the time interval $[0, 1]$.
- **Step 2.** For each planar boundary surface, compute the surface normals (normalized and inward directed). We note that all these normals are constant on the planar surface to which they belong. The normals of edges and vertices will be specified as
 - edge: we assign two normal vectors of two surfaces which intersect at this edge.
 - vertex: we assign all the normal vectors of the surfaces which intersect at this vertex.

From Steps 1 and 2 above, we obtain the normal (or normals) of every boundary point at time 0. It is very easy to compute and check the Tangency Condition $T(\mathbf{x}, t)$ of any point $\mathbf{x} \in \partial M$ at any given time $t \in [0, 1]$ by using formula (1).

By Theorem 3.2, the boundary of the swept volume satisfies the following formula:

$$\partial S_\sigma(M) \subseteq \left\{ \bigcup_{t=0}^1 \partial_0 M(t) \right\} \cup \partial_+ M(0) \cup \partial_- M(1)$$

Here, at each given time instant, $\partial_0 M(t)$ is the set of instantaneous grazing points and $\partial_+ M(0)$ and $\partial_- M(1)$, which are the instantaneous ingress portion and instantaneous egress portion of the boundary at $t = 0$ and $t = 1$, respectively, are both sets of planar patches.

It is quite straightforward to classify any point $\mathbf{x} \in \partial M$ as an ingress point, grazing point, or egress point, according to the definitions we stated in chapter 3.

- **Step 3.** Subdivide the time interval $[0, 1]$ into a finite number of segments which are represented by a sequence of time instants.
- **Step 4.** At time $t = 0$, compute the instantaneous ingress portion of $\partial M(0)$ and discretize it into a finite number of triangular planar patches which are each determined by their three vertices.

For each time instant, do Steps 5, 6 and 7 below. We note that in the 2-D case, our global trimming algorithm is so fast and simple that the local trimming procedure does not seem to be necessary. But in the 3-D case, since the global trimming will be very complicated and require a great deal of computation, the local trimming procedure which is relatively simple and easy, will become very critical in terms of the efficiency of the program.

- **Step 5.** Compute the instantaneous grazing points of $\partial M(t)$.
- **Step 6.** Apply the Local Trimming Procedure proved in Section 2 to eliminate those instantaneous grazing points which are not valid boundary curves.

- **Step 7.** At time $t = 1$, compute the instantaneous egress portion of $\partial M(1)$ and discretize it into a finite number of triangular planar patches which are represented by their three vertices.
- **Step 8.** Collect all those points obtained in steps 4, 5 and 6 and organize them into groups of points belonging to surfaces. These are the candidate boundary surfaces.
- **Step 10.** Global trimming: Due to the global nature of the general sweep, we need to eliminate those candidate points which belong to the interior of the swept volume $S_\sigma(M) = \bigcup_{t=0}^1 M(t)$. As in the 2-D case, this will include initial global trimming and secondary global trimming
- **Step 11.** Connect the remaining candidate points to form a set of boundary triangular patches which comprise a polyhedral approximation of the boundary representation of the swept volume.
- **Step 12.** Use the output of the previous steps and various graphics techniques to produce realistic visualizations of the swept volume which can be viewed from different perspectives.

CHAPTER 6

CONCLUSIONS

In this thesis, we studied the problem of obtaining the boundary representation of a swept volume generated by a rigid object undergoing a smooth, but otherwise general sweep. By using the sweep differential equation to characterize the sweep, we developed a very general evaluation procedure which is comprised of the following basic steps: First, classify the boundary points of the sweeping object based on their relationship with the sweep flow field, and thus produce a set of candidate boundary patches. Then, apply a local trimming operation to remove some of the candidate boundary points which are not members of the boundary of the swept volume. Finally, due to the global nature of the general sweep, a global trimming procedure is needed to remove the remaining candidate boundary patches (or portions of candidate boundary patches) which belong to the interior of the swept volume. The final boundary representation of the swept volume is then formed by the boundary patches. We have devised a general global trimming criterion which theoretically identifies valid boundary patches in an efficient manner. Our general global trimming criterion includes both initial global trimming and secondary trimming; secondary global trimming is used to deal with singular cases that seem to have escaped the attention of some research.

Based on the general evaluation procedure, 2-D prototype software which incorporates a very efficient 2-D global trimming algorithm has been developed. The program produces good approximations to the boundary of the swept volume of any planar polygonal object undergoing a general smooth sweep. Although it is clear that the precision of the approximation can be controlled by adjusting the partition of the time interval and also by selecting the method to connect the boundary points, we

have not yet made a thorough error analysis. Compared with other programs, our method seems to be more efficient and general; for example, it readily handles cases in which the boundary of the swept volume has more than one component. We also tested the program on shapes for which the object boundary is not a polygon, e. g. , a circle, by using polygonal approximation. However, the relationship between the precision of polygonal object approximation and the precision of the resulting swept volume approximation, and how to control the approximation of the object for more general shapes, etc., need further study.

The application of the general process to the 3-D case, which is very similar to the 2-D case but certainly will be much more complicated, is also briefly described. To actually develop the 3-D prototype software, many interesting problems await further research: e. g., rapidly computing the grazing curves, devising an efficient 3-D global trimming algorithm, and combining the sweep differential equation theory with computer graphics techniques in order to obtain realistic renderings of swept volume which can be employed to advantage in manufacturing engineering practice.

APPENDIX A: PROOF OF THE ALGORITHM 4.1

A proof of a part of this result is outlined in the exercises in [9]. We first recall the definition of the mod 2 degree of a map. Let X and Y be closed, n -dimensional manifolds and

$$f : X \rightarrow Y$$

a continuous mapping. It is well-known(see [21]) that for any $x \in X$, the n th homology group with coefficients in \mathbf{Z}_2 , the field of integers modulo 2, satisfies

$$H_n(X, X \setminus x; \mathbf{Z}_2) \approx \mathbf{Z}_2$$

The map f induces a map of homology groups.

$$f_* : H_n(X, X \setminus x; \mathbf{Z}_2) \rightarrow H_n(Y, Y \setminus f(x); \mathbf{Z}_2)$$

that yields a map

$$f_* : \mathbf{Z}_2 \rightarrow \mathbf{Z}_2$$

by making the usual identifications. The *mod 2 degree* of f is defined to be

$$\deg_2 f = f_*(1)$$

Let us now assume that X is piecewise smooth, Y is smooth and $f : X \rightarrow Y$ is continuous and piecewise smooth. A point $y \in Y$ is a *regular value* of f if

$$f^{-1}(y) = \{x \in X : f(x) = y\}$$

consists only of points at which f is smooth and the derivative $Df(x)$ is invertible. By compactness, it follows that $f^{-1}(y)$ is finite if y is a regular value(see [9] and [13]) and

$$\deg_2 f = \#f^{-1}(y) \pmod{2}$$

In addition, Sard's Theorem implies that the set of regular values is dense in Y , so any y can be perturbed to a regular value.

We now further restrict X by assuming that it is a polyhedron that is imbedded in \mathbf{R}^{n+1} as a closed, n -dimensional submanifold that is homeomorphic to the n -sphere S^n . By the Jordan–Brouwer Separation Theorem (see [9], [13] and [21]), X has an inside and outside. If $x_0 \in \mathbf{R}^{n+1} \setminus X$, there is a simple method based on degree theory for deciding if x_0 is inside or outside X . Let $S_\epsilon(x_0)$ be a small n -sphere of radius $\epsilon > 0$ that is centered at x_0 and does not intersect X . We can map X into $S_\epsilon(x_0)$ by radial projection along rays emanating from x_0 . For $x \in X$, this map is easily seen to be defined by

$$f(x) = x_0 + \frac{\epsilon(x - x_0)}{\|x - x_0\|}$$

The radial projection

$$f : X \longrightarrow S_\epsilon(x_0)$$

is clearly continuous and piecewise smooth. In fact, it only fails to be smooth at faces of dimension less than n of the polyhedron X . Standard degree theoretical results imply that x_0 is inside X iff $\deg_2 f \neq 0$.

It is easy to characterize the regular values of the radial projection f as follows: $y \in S_\epsilon(x_0)$ is regular iff the ray from x_0 through y does not intersect any edges of the polyhedron X . At this point, a proof of Algorithm 4.1 is easily within reach, and it should be noted that there is also a rather obvious generalization to polyhedral objects in any \mathbf{R}^n .

Let $x_0 \in \mathbf{R}^2 \setminus \partial M(t)$ and X be the 1-dimensional polygonal closed curve $\partial M(t)$. Draw a ray from x_0 in any direction. If this ray does not intersect a vertex of X , the corresponding point $y \in S_\epsilon(x_0)$ is a regular value of the radial projection

$$f : \partial M(t) \longrightarrow S_\epsilon(x_0)$$

If the ray has an odd number of intersections with $\partial M(t)$, then $\deg_2 f \neq 0$ and x_0 is inside of $\partial M(t)$ according to the criterion established above. On the other hand, when the number of intersections is even, $\deg_2 f = 0$, and x_0 must lie outside of $\partial M(t)$. The special case 1.1, 1.2, 2.1 and 2.2 correspond to situations where y is not a regular value. A small perturbation of y , however, produces an arbitrarily close regular value since the regular values are dense. Observe that a small rotation of the ray in case 1.1 yields an intersection with one less edge and this adds one to the count modulo 2. For case 1.2, a small perturbation produces an intersection with either the same number of edges or two fewer edges, and this adds zero to the count modulo 2. Cases 2.1 and 2.2 clearly yield to the same perturbation analysis, and thus the proof is complete.

REFERENCES

- [1] Baumgart, B. 1972. "Winged-based Polyhedron Representation." *Stanford Intelligence Report No. CS-320*.
- [2] Blackmore, D., and M. C. Leu. 1990. "Analysis of Swept Volume Via Lie Groups and Differential Equations." *Int'l. J. of Robotics Research* (to appear).
- [3] Blackmore, D., and M. C. Leu. 1990. "A Differential Equation Approach to Swept Volumes." *Proc. Rennselaer's Second Int'l Conf. on Computer Integrated Manufacturing*. Troy:143-149.
- [4] Blackmore, D., and M. C. Leu. 1991. "Sweep Differential Equation Analysis of Multiaxis NC Machining." (preprint).
- [5] Blackmore, D., M. C. Leu, and K. K. Wang. 1992. "Application of Flows and Envelopes to NC Machining." *Annals of the CIRP*.
- [6] Boltyanskii V. G. 1964. *Envelopes*. Macmillan, New York.
- [7] Christenson, C. O., and W. L. Voxman. 1977. *Aspects of Topology*. New York: Marcel Dekker.
- [8] Drysdale, R., R. Jerard, B. Schaudt, and K. Hauck. 1989. "Discrete Simulation of NC Machining." *Algorithmica*, 4:33-60
- [9] Guillemin, Vector, and A. Pollack. 1974. *Differential Topology*. Prentice-Hall, Inc., Englewood Cliffs, New Jersey.
- [10] Jerard, R., and R. Drysdale. 1991. "Method for Geometric Modeling, Simulation and Spatial Verification of NC Machining Programs." *Product Modeling for Computer Aided Design*. Amsterdam, North Holland, 1-14.
- [11] Kedem, G., R. Marisa, J. Menon, and H. Voelcker. 1990. *Ray Representation for Swept and Offset Solids*. Tech. Report CPA 90-2, College of Engineering, Cornell University.
- [12] Leu, M. C., S. Park, and K. K. Wang. 1986. "Geometric Representation of Translational Swept Volume and its Applications." *ASME J. of Engineering for Industry*. 108:113-119.
- [13] Milnor, J. 1965. *Topology from the Differentiable Viewpoint*. University Press of Virginia, Charlottesville.

- [14] Munkres, J. R. 1961. *Elementary Differential Topology*. Princeton University Press, Princeton, New Jersey.
- [15] Narvekar, A. P. 1991. *Representation and Application of Swept Solids for Numerically Controlled Milling*. Master's Thesis, Department of Mechanical and Aerospace Engineering, State University of New York at Buffalo, Buffalo, NY.
- [16] Requicha, A. A. G. 1977. "Constructive Solid Geometry." *Technical Memo 25*, Production Automation Project, University of Rochester, Rochester, NY.
- [17] Requicha, A. A. G. 1977. "Mathematical Models of Rigid Solid Objects." *Technical Memo TM-28*. Production Automation Project, University of Rochester, Rochester, NY.
- [18] Requicha, A. A. G. 1980. "Representation of Rigid Solids: Theory, Methods and Systems." *ACM Computing Survey*. 12(4):437-464.
- [19] Requicha, A. A. G., and H. B. Voelcker. 1982. "Solid Modeling: a Historical Summary and Contemporary Assessment." *IEEE Computer Graphics and Applications*. 2:9-14.
- [20] Sambandan, K. *Geometry Generated by Sweeps of Polygons and Polyhedra*. Tech. Report 66, Injection Molding Project, College of Engineering, Cornell University.
- [21] Spanier, E. 1966. *Algebraic Topology*. McGraw-Hill, New York.
- [22] Sungertekin, U., and H. Voelcker. 1986. "Graphical Simulation and Automatic Verification of NC Machining Programs." *Proc. IEEE Int'l. Conf. on Robotics and Automation*: 157-165.
- [23] Wang, W. P., and K. K. Wang. 1986a. "Real-time Verification of Multi-axis NC Programs with Raster Graphics." *Proceeding of 1986 IEEE Int'l Conference on Robotics and Automation*: 166-171.
- [24] Wang, W. P., and K. K. Wang. 1986b. "Geometric Modeling for Swept Volume of Moving Solids." *IEEE Computer Graphics and Applications*. 6(12): 8-17.
- [25] Weld, J. D., and M. C. Leu. 1990. "Geometric Representation of Swept Volume with Application to Polyhedral Objects." *Inter'l Journal of Robotic Research*. 9:105-107.

- [26] Wilson, E. B. 1911. *Advanced Calculus*. Dover Publication INC., NewYork.
- [27] Weiler, K. 1985. "Edge-Based Data Structures for Solid Modeling in Curved-Surface Environment." *IEEE Computer Graphics and Applications*. 1: 21-40.